CHAPTER 3

DEVELOPMENT AND EVALUATION OF CLOBETASOL PROPIONATE LOADED LIPID-POLYMER HYBRID NANOPARTICLES

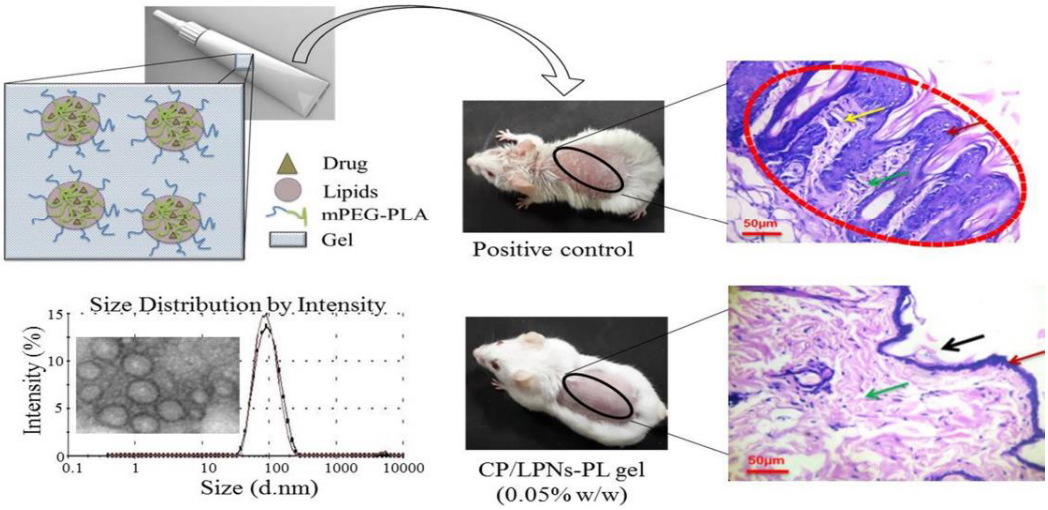

- **Introduction**
- **Experimental section**
- **Results**
- **Discussion**
- **Conclusion**

1. Introduction

Psoriasis is an immune-mediated, chronic, non-contagious disease of the skin that involves a series of cellular changes resulting in skin erythema, thickened silver scaly plaques, hyperkeratosis, vascular angiogenesis, abnormal differentiation and hyperplasia of epidermal keratinocytes along with infiltration of various immune cells at the affected site [1-6]. Stress or trauma on epidermal cells activates dendritic cells that lead to the accumulation of macrophages at the affected site by activating T-helper cells resulting in the inflammation-like condition. Macrophages accumulated in the dermal tissue further increases the production of cytokines such as interferon-γ (IFN- γ), tumor necrosis factor (TNF-α), and interleukin (IL) levels that, in turn, activates keratinocytes to undergo proliferation and resultant scale formation. Increased cytokine and other inflammatory mediators also led to angiogenesis by increasing the production of vascular endothelial growth factor (VEGF), leading to the progression of the psoriatic condition [7-10]. Currently, topical corticosteroids are the treatment of choice for symptomatic relief from psoriasis [11-13]. These corticosteroids cause induction of phospholipase A_2 inhibitory proteins, collectively called as lipocortins. These lipocortins control the biosynthesis of prostaglandins and leukotrienes, which are potent mediators of inflammation. In addition to this, corticosteroids bind to the glucocorticoid receptor present in the cytoplasm, thereby forming a drug-receptor complex that enters the cell nucleus and modifies genetic transcription of cytokines and other inflammatory mediators [14, 15]. Clobetasol, a super-potent corticosteroid, is the most frequently prescribed medication for psoriasis. Apart from psoriasis, this drug finds application for treating several dermatological issues ranging from simple eczema to more severe conditions including oral lichen planus, Prurigo nodularis [16], vulvar dermatoses [17], severe erosive gingival lesions [18], vitiligo [19] etc. However its conventional preparations (gels, creams, ointments, etc.)

cause local toxicity (*e.g.*, skin atrophy, skin infections, stretch marks, and redness) and systemic toxicity (*e.g.*, suppression of hypothalamic-pituitary-adrenal (HPA axis)) [20-24]. To avoid these toxicities and improve the efficacy of corticosteroids, new carriers are required that should penetrate deeper into viable epidermis without systemic absorption and release the drug at the local site at a controlled rate over a prolonged period of time.

Nanocarriers have provided viable options wherein drugs could be entrapped in the matrix, thus providing a controlled release and avoiding high loco-regional concentration. Both polymeric and lipidic nanoparticles have shown advantages over conventional systems for topical delivery [25, 26]. Şenyiğit *et al.* made use of lecithin/chitosan nanoparticles to deliver clobetasol propionate topically and found its significant accumulation in the skin as compared to plain chitosan gel and commercial cream [27]. In another study, Silva *et al.* demonstrated improvement in clobetasol propionate penetration in stratum corneum after 6 h, when administered using nanostructured lipid carriers as compared to clobetasol propionate solution [28]. Improved skin penetration and retention were observed for other hydrophobic drugs as well. Sun *et al*. demonstrated that more amount of curcumin penetrated through or accumulated in the psoriatic skin when administered as the curcumin PLGA nanoparticles-loaded hydrogel compared to the free curcumin hydrogel [29]. In another study, Shah *et al.* reported enhancement in the skin permeation of spantide II and ketoprofen to 9.5 and 11.55-fold, respectively, when administered as a nanogel in comparison to free drugs [30]. Apart from nanoparticle mediated improved skin penetration of drug molecules, in a recent work authors have showed that co-encapsulation of clobetasol (CLO) in nanostructured lipid carriers (NLCs) resulted into improved skin penetration (upto 5-fold) of tacrolimus (TAC). The skin permeation of both TAC and CLO was further increased upto 1.8-fold and 1.6-folds by coating these NLCs with chitosan [32].

Although polymeric and lipidic systems offer several advantages over conventional delivery, there is still room for further improvements as certain disadvantages are also associated with these systems as reviewed elsewhere [33]. Lipid-polymer hybrid nano-carriers have been reported to overcome the limitations of polymeric and lipidic nanosystems. Based upon the structure of these nanosystems, they are categorized into a. monolithic, b. core-shell, c. biomimetic lipid-polymer nanoparticles and d. polymer-caged liposomes [33-42]. These newer class of nano-carriers combines advantages of both polymeric and lipidic nano-carriers such as good drug loading capacities, a more controlled drug release, improved cellular uptake, biocompatibility, and stability. Their pharmaceutical applications apart from drug delivery include vaccine adjuvants (for boosting immune response), cancer targeting (docetaxel, paclitaxel, aromatase inhibitor), gene delivery (DNA (pLuc, pEGFP-N2), SiRNA (anti-GFP, anti-Luc and KIF11), and diagnostic (delivering contrast agent such as inorganic nanocrystals and quantum dots (QD) commonly used in magnetic resonance imaging and computed tomography) [43, 44, 34].

Among various lipid-polymer hybrid systems, a monolithic design is simple and scalable yet could achieve most of the benefits of a hybrid system. The reported methods for preparing these hybrid nanosystems are restricted to lab-scale due to the complexity of the process [45-48]. Herein we report a stable and scalable multi-component monolithic lipid-polymer hybrid nanoparticles (LPNs) consisting of a solid lipid, a liquid lipid, and an amphiphilic copolymer. A series of lipids and surfactants were screened to obtain stable LPNs that were able to penetrate the deeper skin tissue, i.e., the viable epidermis. In these LPNs, the hydrophobic block of the amphiphilic copolymer will interact with the lipid core (consisting of solid lipid and liquid lipid) while the hydrophilic block forms a shell around the nanoparticles. Clobetasol propionate, a

highly potent topical corticosteroid, was encapsulated in these LPNs and were subsequently formulated into a topical hydrogel made of carbopol 974P. A thorough *in vitro* evaluation was performed for these LPNs followed by ex-vivo (in psoriatic skin tissue) and *in vivo* assessment for skin penetration, dermatokinetics, systemic absorption, and efficacy in imiquimod induced psoriasis-like skin inflammation in *Swiss albino* mice.

2. Experimental section

2.1. Materials

Clobetasol propionate was received as a kind gift from Orbicular Pharmaceutical Technology Pvt. Ltd. (Hyderabad, India). DL-Lactide, stannous 2-ethyl hexanoate (Sn(Oct)2), methoxy poly(ethylene glycol) (mPEG, Mn 5000), cholesterol, cholic acid and propidium iodide (PI) were procured from Sigma Aldrich (St. Louis, MO). Glyceryl monostearate (GMS), Precirol® ATO5, stearic acid, compritrol ATO 888 were obtained as a gift from Gattefosse, (Lyon, France). Capmul MCM C8 and Captex 355 were provided as a gift from Abitec Corporation (OH, USA). Miglyol®812 was obtained as a gift from CREMER (Hamburg, Germany). Oleic acid and linoleic acid were purchased from Acme Synthetic Chemicals (Mumbai, Maharashtra, India). Tween 80, Span 80 and Solutol HS 15 were obtained as a gift from BASF India Ltd (Mumbai, India). Carbopol 974P was supplied by Lubrizol (OH, USA). Annexin V Alexa fluor 488 conjugate, and SnakeSkin® Dialysis Tubing (3.5 KDa cut-off) were purchased from ThermoFisher Scientific (MA, USA). 3-(4,5-dimethylthiazol-2-yl)-2,5-diphenyltetrazolium bromide (MTT), sodium azide, and sodium lauryl sulfate was purchased from Sisco Research Laboratories (Mumbai, India). 3-(2- Benzothiazolyl)-7-(diethylamino) coumarin was purchased from TCI Chemicals (Tokyo, Japan). Dulbecco's Modified Eagle

Medium (DMEM) and Fetal Bovine Serum (FBS) were obtained from Invitrogen (MA, USA). Dimethyl Sulfoxide (DMSO) and Phosphate Buffered Saline (PBS) pH 7.4 were purchased from HiMedia Laboratories (Mumbai, India). Imiquimod was purchased as Imiquad® (5% w/w; Glenmark, India) from a local vendor. All other reagents and chemicals (analytical grade) were procured from local vendors. Clobetamos™ gel (marketed product) used for comparison was purchased from a local vendor. This product is manufactured by Lyka Labs (Gujrat, India) and is composed of Clobetasol propionate (0.05% w/w), ammonium lactate equivalent lactic acid (12% w/w), methyl paraben (0.2% w/w), propyl paraben (0.02% w/w) and gel base (q.s.). Purified water was collected from a Millipore Direct-Q ultra-pure water system (Millipore, Bedford, USA).

2.2. Synthesis and characterization of mPEG-PLA copolymer

mPEG-PLA copolymer was synthesized by monowave assisted ring-opening polymerization of DL-lactide in the presence of mPEG as a chain initiator and stannous 2-ethyl hexanoate as a catalyst after slight modification of earlier reported methods [49, 50]. Briefly, in a 10 mL microwave specific vial, 0.216 g of mPEG (Mn 5000 Da) was taken and melted at 110 °C for 5 min in the microwave chamber (Monowave 400, Anton Parr, VA, USA). After 5 min, DL-lactide (0.636 g) and stannous 2-ethyl hexanoate (10 mol % of mPEG; in anhydrous toluene) were added to the vial, and ring-opening polymerization was allowed to occur at 110 °C for 30 min in the microwave chamber. Following the completion of the reaction, the crude polymer was dissolved in chloroform, followed by precipitation in cold diethyl ether. The precipitation procedure was repeated twice to yield the purified polymer, which was subsequently dried under vacuum and characterized by ^{1}H-NMR and gel permeation chromatography (GPC). For ^{1}H NMR analysis, mPEG-PLA (25 mg) was dissolved in 600 μL deuterated chloroform ($CDCl_3$) and

characterized using AVANCE II Bruker 400 MHz spectrometer. For gel permeation chromatography, mPEG-PLA (2 mg) was dissolved in chloroform (HPLC grade) and analyzed using Waters 515 HPLC system equipped with Styragel® columns (HR4, 300 mm x 7.8 mm) with molecular weights range: 5kDa-600kDa connected in series with a differential refractive index detector (Waters 2414). Polystyrene of different molecular weights (3.26, 5.27, 12.0, 26.6, 50.0, and 120.0 KDa) were used as standards for comparison, and data were analyzed by Breeze 2 software.

2.3. Preparation and characterization of lipid-polymer hybrid nanoparticles (LPNs)

Clobetasol propionate loaded LPNs (CP/LPNs) were initially prepared at a batch size of 0.184 g with different combinations of solid lipid, liquid lipid, and surfactant to study their effect on particle size and encapsulation efficiency. As shown in Table 1, amphiphilic polymer mPEG-PLA (molecular weight: 12927 Da), solid lipids (Precirol® ATO5, Glyceryl monostearate (GMS), Comptritol®, Stearic acid, Cholesterol, and Cholic acid), liquid lipids (Linoleic acid, Oleic acid, Miglyol®, Capmul MCM C8, Captex 355) and surfactants (Span 80, Tween 80 and Solutol HS 15) were screened to obtain stable CP/LPNs with desired particle size (< 200 nm), narrow polydispersity index (PDI) (<0.3) and encapsulation efficiency (>80%). Briefly, clobetasol propionate (4 mg), solid lipid (60 mg), liquid lipid (60 mg), and mPEG-PLA copolymer (60 mg) were dissolved in chloroform (800 μL) in a 5 mL glass vial by slight warming to 40ºC. The solution was then heated at 70 °C for 2 h to remove the chloroform. The homogeneous hybrid matrix obtained was cooled to room temperature, followed by the addition of purified water (3 mL) containing tween 80 (1.5% w/v). The crude suspension was subjected to probe sonication (4 min/ 25% amplitude) followed by centrifugation at 5000 rpm for 5 min. The

supernatant containing CP/LPNs was collected and analyzed for particle size, PDI, and zeta potential (Malvern Nano ZS).

CP/LPNs were then prepared at a batch size of 4.9 g with two selected compositions. Batch 1 (CP/LPNs-GO) consisted of clobetasol propionate (0.107 g), glyceryl monostearate (solid lipid; 1.6 g), Oleic acid (liquid lipid; 1.6 g) and mPEG-PLA (1.6 g, molecular weight: 12927 Da) copolymer and batch 2 (CP/LPNs-PL) consisted of consisting of clobetasol propionate (0.107 g), Precirol®ATO 5 (solid lipid; 1.6 g), linoleic acid (liquid lipid; 1.6 g) and mPEG-PLA copolymer (1.6 g; molecular weight: 12927 Da). All constituents were dissolved in chloroform (7 mL) by slight warming to 40 ºC in a 100 mL beaker. Chloroform was then removed by heating at 70 ℃ for 3 h to form a homogenous hybrid matrix. The matrix was cooled to room temperature, and to this, purified water (50 mL) containing tween 80 (1.5% w/v) was added, followed by high shear homogenization at 30,000 rpm for 5 min to obtain a coarse dispersion. This coarse dispersion was then subjected to size reduction using high-pressure homogenization (Panda Plus, GEA Niro Soavi, Italy) at 1000 bars for 5 min at a temperature below 45ºC. The nanodispersion obtained was immediately cooled down on an ice bath to obtain the CP/LPNs that were centrifuged at 5000 rpm for 5 min to remove the unentrapped drug and coarse particles. The supernatant containing CP/LPNs was collected and analyzed for particle size and encapsulation efficiency, as stated earlier. The presence of residual chloroform was analyzed using a Shimadzu GC (model number GC-2010 Plus) equipped with an oven with temperature programming capability, flame ionization detector (FID), and a Shimadzu HS-10 autosampler. Data acquisition and processing were accomplished using GC solutions software. The morphology of prepared CP/LPNs was determined using Field Emission-Scanning Electron Microscopy, FE-SEM (FEI Quanta FEG 250 SEM, Hillsboro, Oregon, Washington) and High

Resolution-Transmission Electron Microscopy, HR-TEM (TECNAI 200 Kv TEM, FEI Electron Optics, Eindhoven, Netherlands). Further, the CP/LPNs and blank LPNs dispersion were lyophilized (FreeZone Triad® Benchtop Freeze Dryers (Labconco, MO, USA)) and were characterized using FTIR spectrometer (Bruker Apha, MA, USA) and Differential Scanning Calorimeter (DSC 4000 System, 100-240V/50-60Hz, CT, USA). For lyophilization, no cryoprotectants were included. The formulation i.e. nanoparticle dispersion and gel containing nanoparticles were frozen at -80°C overnight and subjected to vacuum at 0.151mBar for 1 day at -55°C.

2.4. Preparation and characterization of CP/LPNs containing gel (CP/LPNs gel)

CP/LPNs-GO or CP/LPNs-PL gel (equivalent to 0.05% w/w of clobetasol propionate; 100 g) was prepared using carbopol 974P (0.75% w/v). Briefly, carbopol 974P (0.75 g) was hydrated with purified water (10 mL) for 10 h followed by the addition of freshly prepared CP/LPNs (equivalent to 0.05 g of clobetasol propionate) and mixed to obtain a uniform dispersion. Propylene glycol (13 g), methylparaben (0.3 g) and propylparaben (0.3 g) were added to the above mixture and stirred vigorously until visual homogeneity was obtained. Purified water was then added to make up the weight to 95 g, and the pH of the mixture was adjusted to 6.8 with sodium hydroxide (1 M) to obtain a gel. Purified water was then added to make up the weight to 100 g and mixed well to obtain a visual homogeneity. The morphological evaluation of the CP/LPNs-PL in the gel was determined using FE-SEM and HR-TEM to confirm the integrity of CP/LPNs-PL after formulating it into a topical gel. The rheological measurement of the CP/LPNs-PL gel (250 mg) was determined using a Rheometer (MCR 92, Anton Paar, Germany). Briefly, a parallel plate with a diameter of 25 mm was used, and a gap between the probe and plate was kept at 0.5 mm. The shaft was rotated at a shear rate of 10 s^{-1} for 3 min with an

equilibration time of 9 s at 25 °C, and corresponding viscosities (cP) at 20 time points were measured. The average of the last three viscosity values was taken and reported as viscosity (cP) of the final product. The rheological behavior of CP/LPNs-PL gel was studied by continuous shear investigations to evaluate the shear rate (1/s) as a function of shear stress (mPa). Shear rate was varied from 0.1 s^{-1} to 100 s^{-1} with a total 180 point number, and the corresponding shear stress (mPa) was measured at 25 °C.

2.5. In vitro drug release studies

In vitro clobetasol propionate release from CP/LPNs-GO and CP/LPNs-PL gel was carried out using a most widely used dialysis bag method [51]. Dialysis bag (3.5 KDa cut-off; SnakeSkin® Dialysis Tubing, ThermoScientific) containing the free clobetasol propionate (free CP), a gel containing free clobetasol propionate (CP gel) or CP/LPNs (CP/LPNs-GO and CP/LPNs-PL) gel were placed in a 30 mL of release media consisting phosphate buffer saline (pH 7.4) containing sodium lauryl sulfate (1% w/v), sodium azide (0.2% w/v) and ethanol (2% v/v). Samples were kept in an incubator at 37ºC, and aliquots were taken at regular time intervals *viz.* 15 min, 0.5 h, 1 h, 2 h, 4 h, 8 h, 12 h, 1 day, 3 day, 5 day, and 7 day. The amount of clobetasol propionate in the release samples was determined by RP-HPLC method, and cumulative release was plotted against time. The drug release kinetics were determined after fitting the drug release data in various kinetic models using the DDSolver software program.

2.6. Stability studies

The CP/LPNs-PL gel was stored at cool conditions (2-8 °C) and ambient temperature for 6 months in aluminum collapsible tubes. Samples were collected after 3 and 6 months for visual observation (for syneresis, consistency, and grittiness), drug content analysis, and *in vitro*

clobetasol propionate release study. For drug content analysis, 150 mg of CP/LPNs-PL gel was mixed with acetonitrile (1.2 mL) in microcentrifuge tubes and heated at 70 °C till a clear solution was obtained. The sample was further sonicated using a bath sonicator to extract the drug. Samples were then centrifuged at 17,500 rpm for 10 min, and the supernatant was analyzed by RP-HPLC method. The *in vitro* drug release of stability samples were performed in a similar way as given above for CP/LPN gels. The difference (*f1*) and similarity factor (*f2*) of the drug release profiles were determined using DDSolver software [52].

2.7. In vitro cell culture studies

2.7.1. Cellular uptake

The *in-vitro* cell-based assays were carried out on HaCaT cells as they mimic the hyperproliferative and impaired differentiation condition of psoriatic epidermal keratinocytes [53]. HaCaT cells were obtained as a kind gift from Dr. Munia Ganguly, CSIR-IGIB, New Delhi. The cells were cultured in Dulbecco's Modified Eagle's Medium (DMEM) supplemented with 10% fetal bovine serum (FBS; HyClone, Logan, UT) containing 1% antibiotics and kept in an incubator at 37 °C/ 5% CO_2 (Forma™ Series 3 Water Jacketed CO2 Incubator, Thermo fisher scientific). To evaluate the cellular uptake, coumarin-6 (C6), a green fluorescent hydrophobic dye was loaded in the LPNs. Briefly, cells were seeded at a cell density of 1×10^5 cells/well in 6-well cell culture plates, allowed to adhere for 24 h followed by treatment with free C6 or C6/LPNs. The cellular uptake was determined after 4 h treatment by flow cytometry and fluorescence microscopy. For flow cytometry, cells were washed thrice with PBS, trypsinized, centrifuged (1200 rpm/3 min at 4ºC) and cell pellet obtained was resuspended in 0.5 mL cold PBS followed by flow cytometric analysis (Cytoflex, Beckman Coulter, USA). The C6 was

excited with an argon laser at 488 nm, and fluorescence was measured at 525 nm. Data were analyzed using CytExpert and FlowJo softwares. For fluorescence microscopy, cells were washed thrice with PBS, fixed using Paraformaldehyde solution (4% v/v), washed with PBS, and counterstained with DAPI (300 nM) followed by analysis using a fluorescence microscope (Axio Vert. A1 FL, Carl Zeiss, Jena, Germany).

To elucidate the cellular uptake pathway, the HaCaT cells were pretreated for 1 h with endocytosis inhibitors at their non-toxic concentration i.e. methyl-β-cyclodextrin (MβCD; 20 mM), mycostatin (MST; 150 μM), chlorpromazine (CPZ; 10 μg/mL) and amiloride (AMD; 10 mM). These inhibitors were reported to block lipid-raft mediated endocytosis, caveolae-mediated endocytosis, clathrin-mediated endocytosis, and macropinocytosis, respectively [54-56]. After pre-incubation with the inhibitors, free C6 or C6/LPNs were added to the wells and incubated for 4 h followed by flow cytometry and fluorescence microscopy analysis as given above.

2.7.2. In vitro cytotoxicity assay

Cell growth inhibition potential of CP/LPNs-PL was performed in HaCaT cells using MTT assay [57]. Briefly, $5x10^3$ cells/well were seeded in 96-well cell culture plates and incubated at 37 °C/ 5% CO_2 for 24 h. Cells were then treated with free clobetasol propionate (CP) or CP/LPNs-PL at concentrations ranging from 1 to 100 μM equivalent to clobetasol propionate and blank LPNs-PL. After 48 h, the culture media was removed, plates were washed with sterile PBS (pH 7.4), and fresh serum-free media containing 3-(4,5-dimethylthiazol-2-yl)-2,5-diphenyltetrazolium bromide (MTT; 5mg/mL) was added to each well. After 4 h, the media were removed, cells were washed with PBS, and formazan crystals were dissolved in molecular grade dimethyl sulphoxide. The absorbance was recorded at 560 nm by using a microplate reader

(BioTek Epoch) and corrected for the cell debris by subtracting the absorbance at 630 nm from the absorbance at 560 nm. The cell viability was determined by comparison with untreated cells using the following formula.

$$\% \text{ Cell viability} = (\text{OD sample wells}/ \text{OD control wells}) \times 100$$

2.7.3. Apoptosis assay

HaCaT cells (1 x 10^6 cells/well) were seeded in 6-well cell culture plates and incubated at 37 °C/ 5% CO_2 for 24 h. The cells were treated with blank LPNs-PL, free clobetasol propionate, or CP/LPNs-PL at a concentration equivalent to 100 μM of clobetasol propionate. After 48 h, cells were washed with sterile PBS (pH 7.4), trypsinized, centrifuged (2000 rpm/5 min) and resuspended in 1X binding buffer. Annexin V-FITC conjugate and propidium iodide were used to quantify the cellular apoptosis using flow cytometry as per the supplier's protocol (ThermoFisher Scientific, USA). A total of 10,000 cells were analyzed by flow cytometry (Cytoflex, Beckman Coulter, USA) and data were interpreted using CytExpert version 2.0, (Beckman Coulter software).

2.7.4. Cell-cycle analysis

HaCaT cells (2 × 10^5 cells/well) were seeded in 6-well cell culture plates and incubated at 37 °C/ 5% CO_2 for 24 h. After 24 h, cells were treated with blank LPNs-PL, free clobetasol propionate, or CP/LPNs-PL at a concentration equivalent to 100 μM of clobetasol propionate for 48 h. Post-treatment, the media was aspirated, and cells were washed twice with PBS, followed by trypsinization. The cells were harvested by centrifugation (1200 rpm/ 3 min), suspended in 1 mL of 70% ethanol (precooled at −20 °C) for 20 min followed by staining with propidium iodide

and analyzed using flow cytometer (Cytoflex, Beckman Coulter, USA). Data were interpreted with CytExpert software version 2.0 (Beckman Coulter software).

2.8. Ex vivo and *in vivo* assessment of CP/LPNs gel

2.8.1. Establishment of imiquimod-induced psoriasis-like skin inflammation in Swiss albino mice

Imiquimod (IMQ), a potent immune activator, was used to develop psoriasis-like skin inflammation in *Swiss albino* mice [58]. All animal experiments were approved by the Institutional Animal Ethics Committee (IAEC) (protocol no: IAEC/RES/25/10, IAEC/RES/25/11 and IAEC/RES/26/05), and studies were performed as per CPCSEA guidelines. Animals were acclimatized for one week prior to experimentation and housed in plastic cages under standard laboratory conditions with 12 h dark and 12 h light cycle. Psoriasis was induced in *Swiss albino* mice (8 to 12 weeks old) by topical application of commercially available IMQ cream (62.5 mg; 5%) on the shaved back and right ear for five consecutive days, translating to a daily dose of 3.125 mg of IMQ. An objective scoring system based on the clinical Psoriasis Area and Severity Index (PASI) was used to access the development of psoriasis wherein erythema, scaling and thickening were scored independently on a scale from 0 to 4 with a score of 0 as none; 1 as slight; 2 as moderate; 3 as marked and 4 as very marked. Cumulative scoring (erythema plus scaling plus thickening) was done on a scale from 0 to 12 indicated the extent of inflammation [59, 60].

2.8.2. Ex vivo bioimaging

Coumarin-6 (C6) dye a common fluorescent marker was used to examine the ex *vivo* distribution of LPNs in the psoriatic skin of *Swiss albino* mice [61]. Herein, C6 dye was loaded in the LPNs using a similar preparation method as that of CP/LPNs-PL. The shaved psoriatic

skin of *Swiss albino* mice was mounted between the donor and receptor compartment that was held tightly by clamps in Franz diffusion cells with the contact surface area of 1 cm^2. The receptor compartment was filled with PBS (5 mL; pH 7.4) containing ethanol (2% v/v). In the donor compartment, free coumarin-6 (C6) and C6/LPNs-PL (equivalent to 2 μg of C6) were taken, followed by incubation for 6 h, 12 h, and 24 h at 37 ± 1 °C at stirring speed of 800 rpm. At each time point, skin samples were unclipped from the Franz diffusion cells and washed three times with PBS (pH 7.4) followed by air drying. A 19 mm Scotch (3M, USA) cellophane tape was used for tape stripping. For the removal of the stratum corneum (SC) layer, 15 strips were detached in such a way that the whole area of the tape was utilized. After removing stratum corneum from skin samples, remaining skin was analyzed by *ex vivo* bioimaging using *In Vivo* Imaging System (IVIS) Lumina XR (Perkin Elmer, UK) at an excitation and emission wavelength of 430 and 510 nm, respectively.

2.8.3. Ex vivo skin permeation studies and estimation of drug in deeper layers of skin

The tape stripping technique was used for quantifying the drug in deeper layers of the skin [62]. In *ex vivo* skin permeation studies for the quantification of CP in deeper dermal layers i.e., viable epidermis and dermis, the skin samples were processed as reported previously with certain modifications [28, 63]. Shaved mice's skin was mounted between the donor and receptor compartment that was held tightly by clamps. The receptor compartment was filled with PBS (5 mL; pH 7.4) containing sodium lauryl sulfate (1% w/v) and ethanol (2% v/v). In the donor compartment, marketed clobetasol propionate gel (Clobetamos™) or CP/LPNs-PL gel (equivalent to 25 μg of clobetasol propionate/cm^2) was taken followed by incubation for 24 h at 37 ± 1 °C with a stirring speed of 800 rpm. After 24 h, aliquots were withdrawn from the receptor

compartment, and skin samples were unclipped from the Franz diffusion cells and washed three times with PBS (pH 7.4) followed by air drying. A 19 mm Scotch (3M, USA) cellophane tape was used for tape stripping. The first stripped tape was discarded as it contains the unabsorbed drug. For the removal of the stratum corneum (SC) layer, 15 strips were detached in such a way that the whole area of the tape was utilized. After removing stratum corneum from skin samples, remaining skin was soaked in methanol and sonicated for 1 h for complete extraction of the drug. The samples were analyzed using developed RP-HPLC method**.**

2.8.4. In vivo systemic absorption after topical application

Swiss albino mice (10 to 12 week old) having imiquimod-induced psoriasis-like skin inflammation were divided into two groups (n = 6) wherein group 1 received 40 mg/cm^2 of Clobetamos™ gel (0.05% w/w, marketed product) and group 2 received 40 mg/cm^2 of CP/LPNs-PL gel (0.05% w/w). At a predetermined time (i.e., 0.5 h, 1 h, 3 h, 6 h, 12 h, and 24 h), blood was withdrawn by retro-orbital plexus, pooled from two animals and plasma was separated by centrifugation at 7000 rpm at 4 °C for 20 min. For group 2, blood was further withdrawn for the next four days, pooled, and similarly, plasma was separated. Clobetasol propionate was extracted from the plasma samples by protein precipitation using acetonitrile.

2.8.5. In vivo efficacy studies

The Swiss albino mice (10 to 12 week old) were divided into five groups (n = 6) with group 1 having healthy animals kept as negative control (kept without any treatment: IMQ or test product) while group 2 to 5 received topical IMQ on both right ear and back skin to induce psoriasis-like skin condition. Group 2 was kept as positive control (treated with only IMQ but no test product); group 3 received 40 mg/cm^2 of marketed clobetasol propionate gel (Clobetamos™

gel; 0.05% w/w); group 4 and 5 were treated with 40 mg/cm^2 of CP/LPNs-PL gel at full-strength (0.05% w/w) and half-strength (0.025% w/w). Treatment was given to all animals for five consecutive days, and efficacy was assessed daily using an objective scoring system that was developed based on the clinical Psoriasis Area and Severity Index (PASI). Ear thickness (both right and left) was measured using a digital micrometer, and back skin thickness was measured using a digital vernier caliper [64, 65]. Animals were sacrificed at the end of the study, and back skin, right ear, spleen, and liver were excised, weighed, and histopathological analysis was performed. For skin samples (right ear and back skin), histopathological parameters like hyperkeratosis, parakeratosis, angiogenesis (capillary proliferation), epidermal hyperplasia, suprapappilary thinning, inflammatory infiltrates, munro microabsess, pustule of Kogoj and total skin damage score (cumulative scoring consisting of addition of all the above parameters) were studied [66, 67]. For the liver, parameters such as infiltration of inflammatory cells, degeneration of hepatocytes, and total liver damage were studied [68]. For spleen, parameters such as depopulation of lymphocytes, the integrity of splenocyte, and total spleen damage were studied. Immunohistochemical *(IHC)* analysis of the back skin of animals was performed to determine the expression of the Ki-67 protein marker and reported as the average number of Ki-67 proteins stained per high power field as reported earlier [69, 64].

2.9. Statistical analysis

Statistical analyses were conducted using GraphPad Prism, version 8 (GraphPad Software, La Jolla, CA, USA). All quantitative data are expressed as mean ± standard deviation (SD) or standard error of the mean (SEM) and significant differences between treatment groups were determined with the student's t-test or ANOVA followed by Tukey's multiple comparison test. A p-value < 0.05 was considered statistically significant.

3. Results

3.1. Preparation and characterization of CP/LPNs and CP/LPNs gel

mPEG-PLA amphiphilic copolymer required for the preparation of LPNs was synthesized *in house* by ring-opening polymerization of DL-lactide in the presence of mPEG as chain initiator. ^{1}H NMR of mPEG-PLA showed the proton peaks for mPEG at δ3.56 (CH_2, m, 4H) and for lactic acid at δ1.6 (CH_3, s, 3H) and δ5.2 (CH, q, 1H). The average molecular weight of the polymer by ^{1}H NMR was found to be 12927 Da while GPC analysis showed the number average molecular weight (Mn) and weight average molecular weight (Mw) to 11790 and 12750 Da, respectively with a PDI of 1.08. CP/LPNs were initially prepared at a batch size of 184 mg and the effects of solid lipids (Glyceryl monostearate (GMS), Precirol® ATO5, stearic acid, compritrol ATO 888, cholesterol and cholic acid), liquid lipids (Oleic acid, linoleic acid, Miglyol®812, Capmul MCM C8 and Captex 355) and surfactants (Tween 80, span 80 and solutol HS 15) on particle size and encapsulation efficiency was determined (Table 3.1). Among different batches, batch 1 (CP/LPNs-GO) and batch 5 (CP/LPNs-PL) showed a particle size 186.6 ± 5.0 nm (PDI 0.35 ± 0.03) and 128.3 ± 1.4 nm (PDI 0.25 ± 0.01), respectively with percentage (%) encapsulation efficiency of 82.1 ± 3.7 and 92.4 ± 3.2, respectively. These batches were further scaled up on high-pressure homogenizer that showed a particle size 96.5 ± 2.1 (PDI 0.27 ± 0.00) and 94.8 ± 7.3 nm (PDI 0.21 ± 0.06), respectively. Further, percentage (%) encapsulation efficiencies were found to be 79.1 ± 0.0 and 84.3 ± 3.9, respectively. These CP/LPNs-PL were further formulated into topical hydrogel using 0.75% w/w carbopol 974P as a gelling agent. The formulation process adopted ensured complete removal of chloroform traces from the prepared CP/LPNs-PL as evident from GC Headspace analysis. HR-TEM and FE-SEM images indicated the spherical shape of nanoparticles (Figure 1C and F). Nanoparticles when

Table 3.1. Composition of LPNs and their characterization for particle size, PDI, zeta potential and encapsulation efficiency (%). In addition to the composition provided, all batches contain clobetasol propionate (4 mg) and mPEG-PLA (60 mg) as amphiphilic copolymer.

Batch No	Solid Lipid	Liquid Lipid	Surfactant	Particle size (nm)	PDI	Zeta potential (-mV)	% Encapsulation efficiency
1	GMS	Oleic acid	Tween 80	186.6±5.0	0.35±0.03	3.1±0.2	82.1±3.7
2	Stearic acid	Oleic acid	Tween 80	267.1±13.1	0.43±0.01	4.1±0.6	60.1±8.3
3	Precirol	Oleic acid	Tween 80	144.8±5.0	0.33±0.06	3.6±0.7	85.6±2.3
4	Cholesterol	Linoleic acid	Tween 80	198.5±7.7	0.37±0.01	1.4±0.1	66.6±0.5
5	Precirol	Linoleic acid	Tween 80	128.3±1.4	0.25±0.01	6.1±0.5	92.4±3.2
6	Cholic acid	Linoleic acid	Tween 80	129.7±13.8	0.24±0.08	7.0±0.3	65.7±2.1
7	Cholic acid	Capmul MCM C8	Span 80	180.7±5.1	0.17±0.02	1.3±1.1	67.4±1.1
8	Cholic acid	Miglyol ®	Solutol HS 15	119.6±5.0	0.39±0.02	1.7±0.2	61.2±0.7
9	Cholic acid	Captex 355	Solutol HS 15	111.1±3.7	0.25±0.01	2.1±0.2	70.6±1.5
10	Precirol	Captex 355	Solutol HS 15	154.5±2.1	0.41±0.02	0.6±0.3	66.5±0.6

incorporated into a topical gel may form aggregates that could impact the therapeutic efficacy. Thus to ensure that there was no aggregation in the LPNs, both FE-SEM and HR-TEM analysis of nanoparticle loaded gel was performed. Results revealed that the shape of the CP/LPNs was retained with no visible aggregation after formulating it into the hydrogel (Figure 3.1D and G). Viscocity (η) of gel containing CP/LPNs-PL was found to be 8322.5 cP at 25 °C under constant shear rate of 10 s^{-1}. Their rheograms revealed a non-newtonian flow behavior characterized by

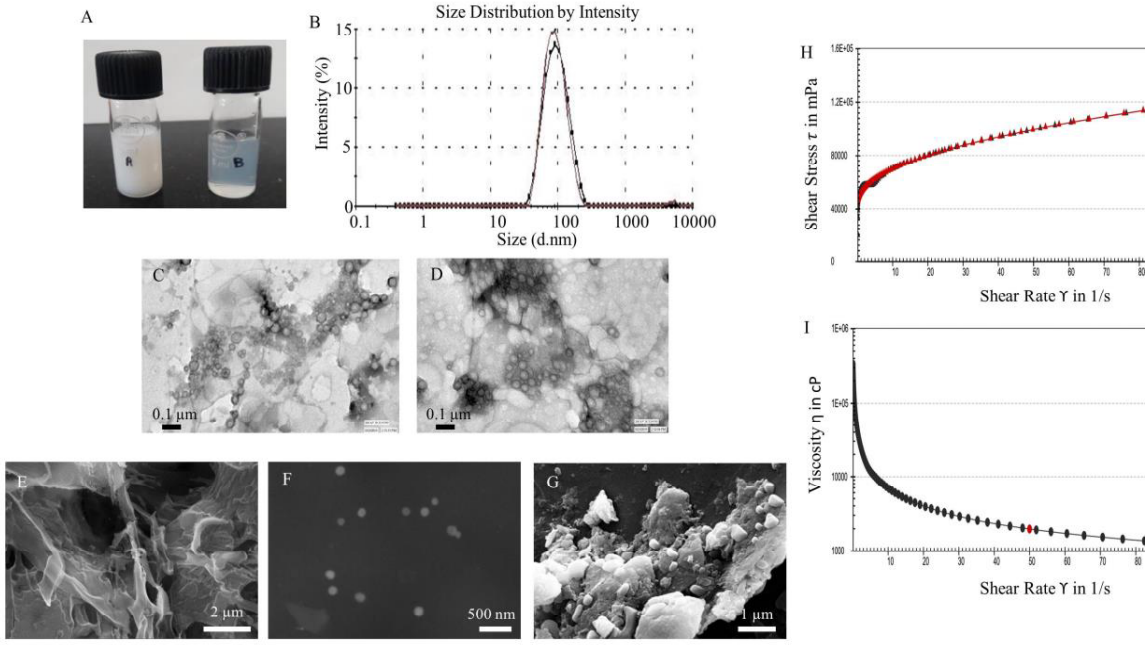

Figure 3.1. Characterization CP/LPNs and CP/LPNs gel. (A) photographic images of undiluted and 100 X diluted CP/LPNs-PL, (B) particle size distribution of CP/LPNs-PL determined by Malvern zetasizer, (C and D) transmission electron microscopic images of CP/LPNs-PL and CP/LPNs-PL gel, (E, F, and G) scanning electron microscopic images of clobetasol propionate loaded gel (CP gel), CP/LPNs-PL and CP/LPNs-PL gel, and (H and I) shear stress versus shear rate and viscosity versus shear rate curves of CP/LPNs-PL gel.

shear-thinning properties with variable thixotropic behavior as evident from viscosity (cP) versus shear rate (1/s) and shear stress (mPa) versus shear rate graphs (Figure 1 H,I). As depicted in (Figure 2A), the FTIR spectra of CP demonstrated its characteristic peaks at 3297 cm^{-1} (O-H stretch), 1732 cm^{-1} (C=O stretch from O-C=O), 1660 cm^{-1} (C=O stretch from O=C-C-Cl), 1605 cm^{-1} (C=C stretch), 1064 cm^{-1}(C-F stretch), 887 cm^{-1} (C-Cl stretch). In case of CP/LPNs and CP/LPNs gel most of the characteristic peaks of drug were disappeared which might be due to the encapsulation of drug inside the core of nanoparticles and low drug to feed material ratio. Further, there was no significant difference between the FTIR spectra of CP/LPNs and CP/LPNs

gel compared to blank LPNs and blank LPNs gel, respectively. In case of CP/LPNs gel and blank LPNs gel, there was slight shifting in the peaks with corresponding reduction in their intensity compared to the CP/LPNs and blank LPNs respectively suggesting that there might be some interaction between the carbopol and nanoparticles. As depicted in (Figure 3.2B), the DSC

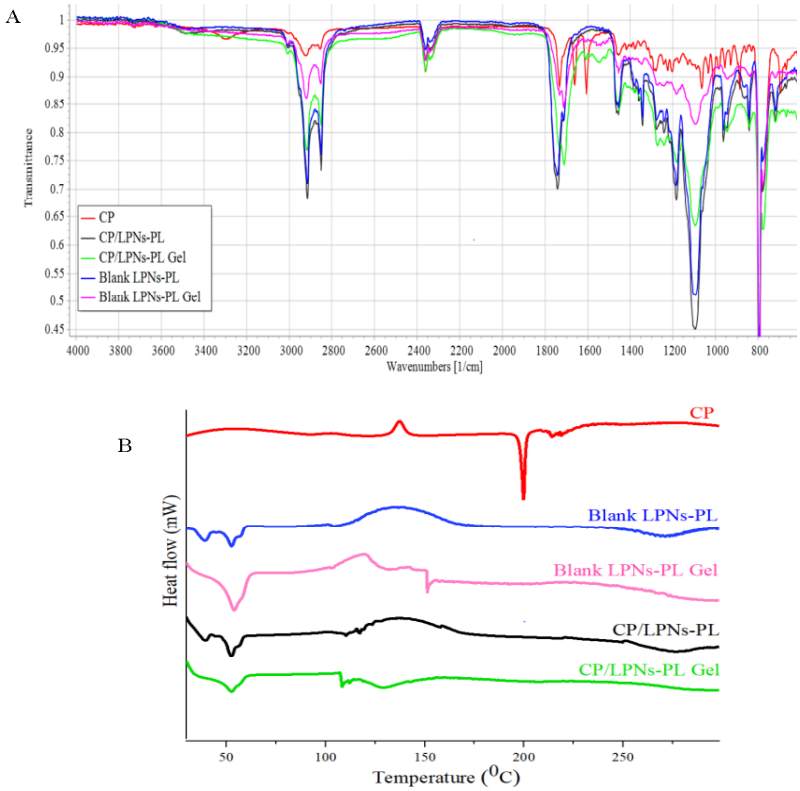

Figure 3.2. (A) FTIR spectra of pure CP, CP/LPNs-PL, CP/LPNs-PL gel, blank LPNs-PL and blank LPNs-PL gel and (B) DSC thermograms of pure CP, blank LPNs-PL, blank LPNs-PL gel, CP/LPNs-PL and CP/LPNs-PL gel.

thermogram of CP demonstrated a sharp endothermic peak at 198 °C, which was the characteristic melting point of drug suggesting its crystalline properties. However, the melting point peak of drug was not observed in the CP/LPNs and CP/LPNs gel suggesting the transformation of drug to amorphous state after encapsulating inside the nanoparticles.

3.2. In vitro drug release studies

A controlled release of clobetasol propionate for 7 days was observed from the CP/LPNs containing gel with CP/LPNs-GO and CP/LPNs-PL prepared using HPH showing a cumulative drug release of 80.2 ± 1.1% and 90.1 ± 0.2% at the end of 7 days (Figure 3.3A). Further, no burst

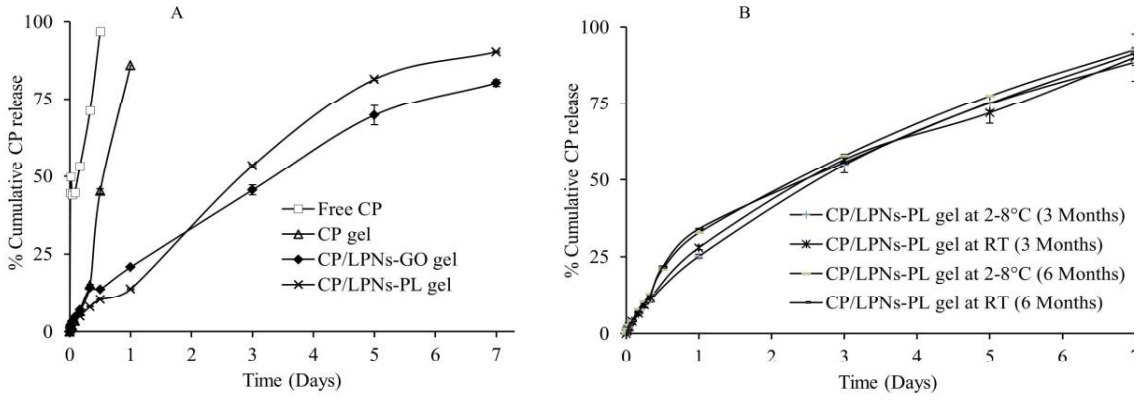

Figure 3.3. *In vitro* release of clobetasol propionate from (A) freshly prepared CP/LPNs gels and (B) CP/LPNs-PL gels stored for 3 months and 6 months at 2-8℃ and room temperature (RT).

release of clobetasol propionate was observed from the CP/LPNs as they showed a cumulative release of 20.8% and 13.7% in one day, respectively, from CP/LPNs-GO and CP/LPNs-PL. Free clobetasol propionate (CP) and gel containing free clobetasol propionate (CP gel) were kept as controls that showed a cumulative drug release of 96.9 ± 0.8% (after 12 h) and 85.9 ± 0.2% (after 24 h), respectively (Figure 3A). Drug release data were fitted into different drug release kinetics models including Zero-order, First-order, Higuchi, Korsemeyer-Peppas, and Hixson-Crowell and it was observed that drug release followed Korsemeyer-Peppas model for CP/LPNs-GO (R^2 = 0.9959) and Hixson-Crowell model for CP/LPNs-PL (R^2 = 0.9927). The n-values obtained from

the Korsmeyer–Peppas model (n = 0.655 for CP/LPNs-GO and n = 0.787 for CP/LPNs-PL) indicated the release mechanism followed anomalous diffusion or non-fickian diffusion.

3.3. Stability studies

CP/LPNs-PL gel was selected and proceeded for stability studies. Stability assessment was conducted at three conditions viz. 2-8 °C, ambient temperature, and accelerated conditions (45°C/75% RH) for 6 months. CP/LPNs-PL gel was found to be stable at room temperature and 2-8 °C for the complete duration of the study with respect to various parameters such as grittiness, syneresis, spreadability, odor, and visual changes. At accelerated storage conditions, syneresis was observed at 3 months. Drug content (%) analysis determined at the end of 3 months and 6 months for the stability samples stored at room temperature was found to be 99.3 ± 0.6 and 98.2 ± 0.2, respectively and that stored at 2-8 °C was found to be 99 ± 0.7 and 97.6 ± 1.1, respectively indicating no degradation of the drug during storage. Gel stored at room temperature and at 2-8 °C for 6 months showed a cumulative drug release of 91.3 ± 0.4% and 92.5 ± 0.6% at the end of 7 days, respectively. *In vitro* drug release profiles of stability samples were found to be similar to that of freshly prepared CP/LPNs-PL gel with no burst release (Figure 3.3B). Difference factor (f_1) for the drug release profiles of samples stored at room temperature and 2-8 °C with respect to freshly prepared samples were found to be 11.62 and 12.22 respectively, while similarity factor (f_2) for the drug release profiles of samples stored at room temperature and 2-8 °C with respect to freshly prepared samples were found to be 66.91 and 67.64 respectively, suggesting that the drug release profiles were identical indicating the stability of gel containing clobetasol loaded LPNs during the study period.

3.4. In vitro cell culture studies

3.4.1. Cellular uptake

Coumarin 6 (C6), a hydrophobic fluorescent dye, was loaded in the LPNs using a similar method as that for CP/LPNs-PL to understand the uptake of nanoparticles in the HaCaT cells which was reported to have an excitation and emission wavelengths of 457 and 501 nm, respectively and thus could be analyzed under FITC filter in fluorescence microscopy study.

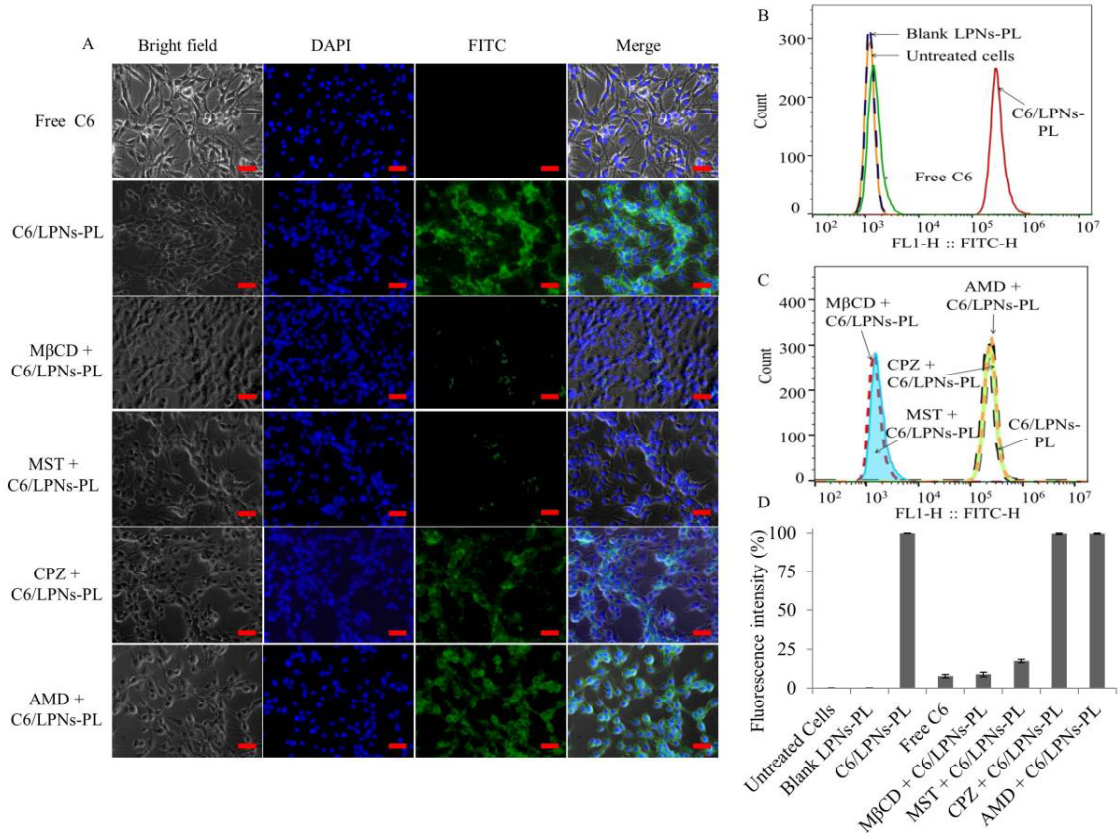

Figure 3.4. (A) Fluorescence microscopy and (B and C) flow cytometry analysis of cellular uptake following incubation with free Coumarin-6 (C6), C6 loaded LPNs–PL (C6/LPNs-PL) and C6/LPNs-PL with various endocytosis inhibitors for 4 h in HaCaT cells (Magnification 40X; Scale bar 200 µm). A visible shift (in B) in the peak (towards right) in C6/LPNs-PL indicating higher internalization while a visible shift (in C) in the peak (towards left) in C6/LPNs-PL plus MβCD or MST indicating lipid raft or caveolin mediated endocytosis, (D) Percent fluorescence intensity of HaCaT cells determined by flow cytometry.

These C6/LPNs demonstrated Z-average particle size (138.03±0.01), PDI (0.194±0.01) and %EE (71.26±2.43). As shown in (Figure 3.4A), it was observed that within 4 h of incubation, C6 loaded LPNs (C6/LPNs-PL) were efficiently taken up by the HaCaT Cells as indicated by the presence of fluorescent green signal while free C6 showed no internalization. The results were quantitatively analyzed by flow cytometry wherein it was observed that 99.81% of HaCaT cells were fluorescent after treatment with C6/LPNs-PL while in free C6 treated cells, only 8.54% showed fluorescence (Figure 3.4D). Further, cells were treated with endocytosis inhibitors including methyl-β-cyclodextrin (Mβ CD), mycostatin (MST), chlorpromazine (CPZ), amiloride hydrochloride (AMD), which suppress lipid raft mediated endocytosis, caveolae-mediated pathways, clathrin-mediated routes and macropinocytosis, respectively. It was observed by both fluorescence microscopy and flow cytometry that MβCD and MST inhibited the uptake of the C6/LPNs-PL. At the same time, CPZ and AMD did not affected the uptake indicating that the internalization was mediated by lipid raft as well as caveolae-mediated pathways.

3.4.2. In vitro cytotoxicity, apoptosis and cell cycle analysis

Cell viability was performed in HaCaT cells after treatment with free clobetasol propionate or CP/LPNs-PL for 48 h. It was observed that CP/LPNs-PL significantly inhibited the cell proliferation of HaCaT cells as compared to free clobetasol propionate (CP) (Figure 3.5B) indicating improved efficacy of clobetasol propionate after encapsulation in the LPNs. Further, blank LPNs-PL i.e. without clobetasol propionate, showed no toxicity to the HaCaT cells. In order to have a mechanistic insight, apoptosis, and cell cycle analysis of HaCaT cells were performed after treatment with the free CP and CP/LPNs-PL. Flow cytometric analysis of

Annexin V-FITC/PI stained cells revealed induction of apoptosis by clobetasol propionate when loaded in LPNs (CP/LPNs-PL) with 12.69% apoptotic cell population (4.47% early and 8.22%

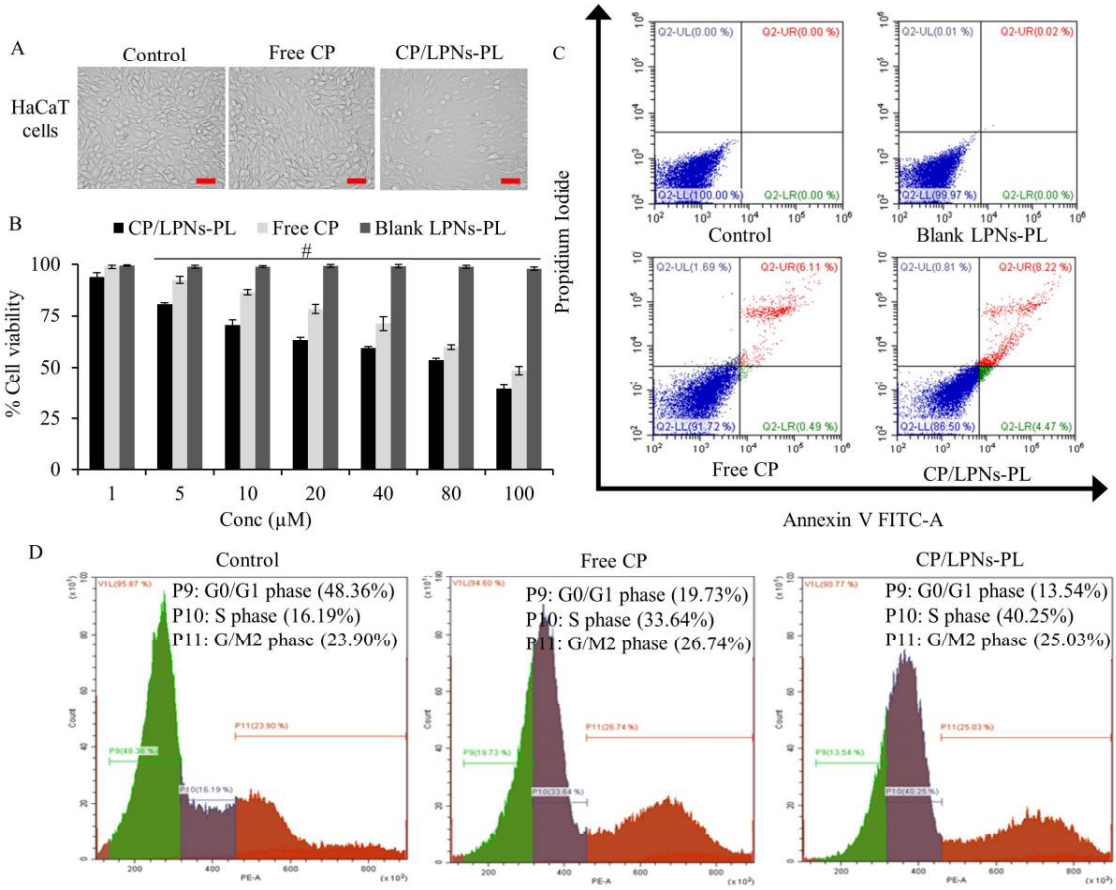

Figure 3.5. (A) Microscopic images of HaCaT cells treated with free clobetasol propionate (CP) and CP/LPNs-PL (Magnification 40X; Scale bar 200 µm), (B, C and D) cell viability, apoptosis and cell cycle analysis of HaCaT cells treated with free CP and CP/LPNs-PL. For cell viability, each value is represented as mean ± SD (n = 4) and statistical analysis was performed using paired *t* test with significant difference of #, $p < 0.01$ free CP versus CP/LPNs-PL.

late stage) as compared to free CP that showed 6.60% apoptotic cell population (0.49% early and 6.11% late stage) (Figure 3.5C). Further, cell cycle analysis revealed significantly higher accumulation of the fraction of cells in synthetic (S) phase when treated with CP/LPNs-PL (40.25%) as compared to free CP (33.64%) (Figure 3.5D).

3.5. Ex vivo bioimaging, skin permeation studies and estimation of drug level in deeper layers of skin

Figure 3.6A, showed the bioimaging of tape stripped *ex vivo* psoriatic skin tissue treated with free C6 or C6/LPNs-PL at 6, 12 and 24 h. Experiment was conducted using *In Vivo* Imaging

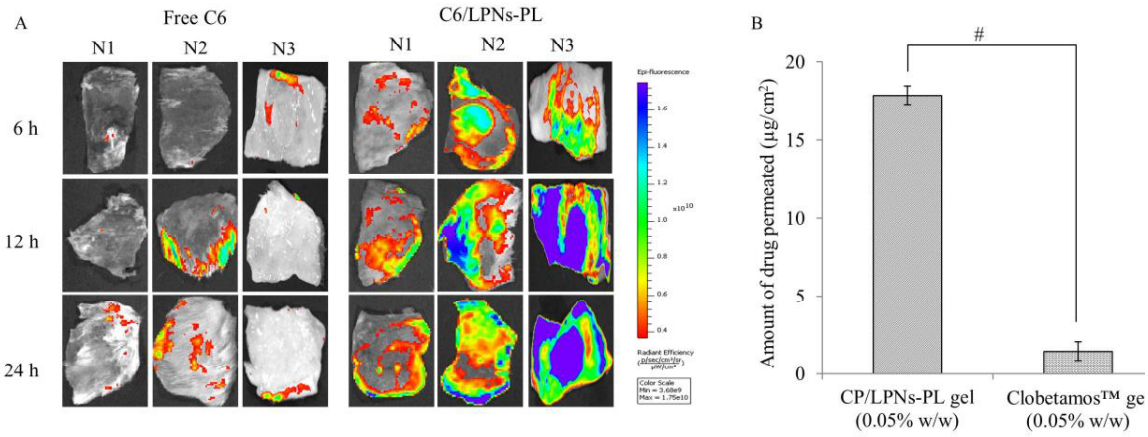

Figure 3.6. Ex vivo permeation of LPNs in psoriatic skin of *Swiss albino* mice. (A) Bio-imaging using IVIS spectrum of *ex vivo* psoriatic skin tissue treated with free C6 and C6/LPNs –PL gel after 6 h, 12 h and 24 h (n = 3) and (B) Quantification of clobetasol propionate in the remaining skin i.e. viable epidermis and dermis after treatment with Clobetamos™ gel and CP/LPNs-PL gel. Each value is represented as mean ± SD. #, $p < 0.01$ versus Clobetamos^{TM} gel (0.05% w/w) group.

System (IVIS) by exciting C6 at 430 nm and recording the corresponding emission at 510 nm. C6/LPNs-PL incubated skin samples showed significantly high fluorescence compared to free C6 incubated skin samples at all the time points suggesting that there was significant improvement in penetration of C6 to deeper skin layers i.e. viable epidermis and dermis when incorporated into the LPNs.

Further, in skin permeation studies, CP/LPNs-PL gel showed no detectable amount of clobetasol propionate in receptor medium that could be correlated to minimal systemic absorption of clobetasol after *in vivo* topical application. The *ex vivo* skin permeation data was

found to be in agreement with the *in vivo* plasma levels of clobetasol propionate obtained after treatment with the CP/LPNs-PL gel as there was no drug detected in plasma samples indicating that CP/LPNs-PL were retained within skin layers and did not enter the systemic circulation. Further, the results obtained for estimation of drug in deeper skin layers suggested that the amount of the clobetasol propionate that have permeated to deeper dermal layers i.e., viable epidermis and dermis was 12-fold higher in case of CP/LPNs-PL gel (17.87 ± 0.03 µg/cm^2) as compared to that of Clobetamos™ gel (1.45 ± 0.61 µg/cm^2).

3.6. In vivo systemic absorption after topical application

Clobetasol propionate, a potent corticosteroid, when applied topically shows undesired systemic absorption exhibiting several side effects including suppression of hypothalamic-pituitary-adrenal (HPA axis) [22-24]. Thus, *in vivo* systemic absorption of clobetasol propionate was determined by analyzing the drug concentration in the plasma after topical application Clobetamos™ gel and CP/LPNs-PL gel. After topical application of Clobetamos™ gel to *Swiss albino* mice, quantifiable levels of clobetasol propionate were observed in the plasma from 30 min to 6 h with a Cmax of 93.81 ± 9.79 ng/mL. On the other hand, animals treated with CP/LPNs-PL gel showed no detectable plasma levels of clobetasol propionate over a period of four days (Table 3.2).

3.7. In vivo efficacy studies

The efficacy of the clobetasol propionate loaded LPNs gel (CP/LPNs-PL gel) was determined in imiquimod-induced psoriasis-like skin inflammation in *Swiss albino* mice. Psoriasis Area Severity Index (PASI) was used to evaluate the effect of the treatment. It was observed that in the positive control group, the erythema, scaling, and thickening started

Table 3.2. Systemic absorption of clobetasol propionate after topical application of Clobetamos™ gel or CP/LPNs-PL gel on the back of IMQ induced psoriatic mice

Time (h)	Clobetamos™ gel (ng/mL)			Average concentration (ng/mL)	CP/LPNs-PL gel (ng/mL)		
	N1	N2	N3		N1	N2	N3
0.5	20.02	56.85	3.95	26.94	**	**	**
1	66.72	102.42	112.31	93.81	**	**	**
3	63.91	77.03	102.07	81.00	**	**	**
6	55.33	30.22	35.84	40.47	**	**	**
12	*	**	*	*	**	**	**

*Detectable but not quantifiable

**Not detectable and not quantifiable

increasing from day one and got progressively increased to a cumulative PASI score of 9.75 on day 5. Treatment groups were able to inhibit the psoriasis progression with a cumulative PASI score of 4, 2, and 0 for Clobetamos™ gel (0.05% w/w; marketed preparation), CP/LPNs-PL gel (0.025% w/w) and CP/LPNs-PL gel (0.05% w/w) treated groups, respectively.

Application of IMQ on right ear and back skin, lead to an increase in the thickness of epidermal tissue due to hyperplasia of keratinocytes and inflammation. In case of positive control group, the average back skin thickness got progressively increased from 1.355 mm (Day 1) to 2.490 mm (Day 5). The back skin thickness were significantly lower for CP/LPNs-PL gel treated group as compared to Clobetamos™ gel treated group. In case of CP/LPNs-PL gel (0.025% w/w) treated group, average back skin thickness was increased from 1.316 mm (Day 1) to 1.574 mm (Day 5) which was comparatively less as compared to Clobetamos™ gel (0.05% w/w) treated group that showed increase in average skin thickness from 1.412 mm (Day 1) to

1.760 mm (Day 5). Similar trends were obtained for change in ear thickness also, as shown in (Figure 3.7). CP/LPNs-PL gel (0.05% w/w) treated group showed least change in the thickness

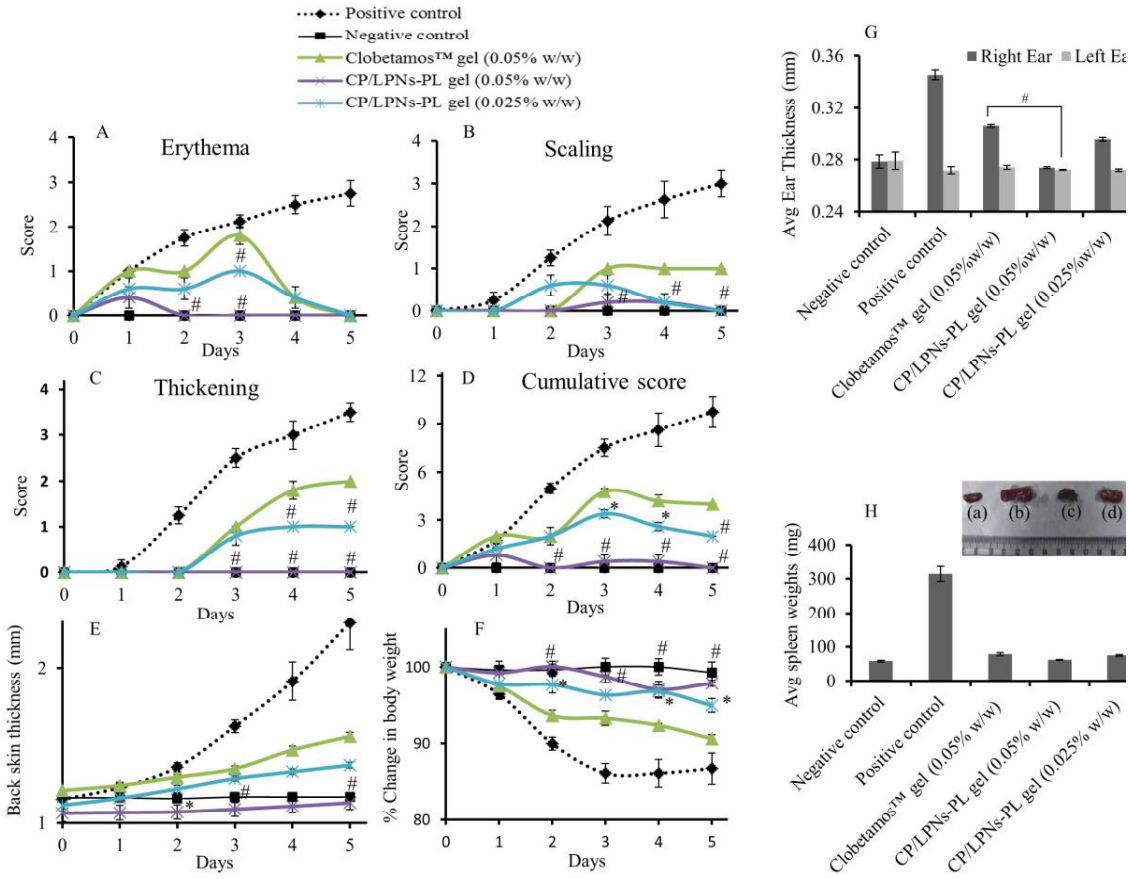

Figure 3.7. CP/LPNs-PL gel inhibited IMQ-induced psoriasis-like skin condition in *Swiss albino* mice (n = 6). (A to C) Scoring of erythema, scaling, and thickening based on the clinical Psoriasis Area and Severity Index (PASI) measured on scale from 0-4, (D) cumulative score indicating the extent of psoriatic inflammation on scale from 0-12, (E) back skin thickness measured using digital vernier caliper, (F) percent change in body weight, (G) Comparative thickness of right and left ear measured using digital micrometer, (H) Average spleen weights for different treatment groups, and comparison of spleen size of treatment groups viz. (a) negative control, (b) positive control, (c) Clobetamos^{TM} gel (0.05% w/w), (d) CP/LPNs-PL gel (0.025% w/w), (e) CP/LPNs-PL gel (0.05% w/w). Each value is represented as mean ± SEM. *, $p < 0.05$ and #, $p < 0.01$, versus Clobetamos^{TM} gel (0.05% w/w) group.

of back skin and right ear and was comparable to that of negative control indicating significant recovery.

The application of IMQ caused the inflammatory condition and resulted in a significant increase in the size and weight of the spleen of positive control animals (314 mg) as compared to the healthy animals (negative control; 58.26 mg). The Spleen weights were significantly reduced on treatment with the Clobetamos^{TM} gel (0.05% w/w), and CP/LPNs-PL gel containing 0.05% and 0.025% w/w of clobetasol propionate. Further, negative control did not show any significant change in body weight throughout the study, while the average body weight of animals in case of positive control group was decreased by 14%. Further, treatment groups, did not show any significant change in body weight compared to Clobetamos^{TM} gel.

3.7.1. Histopathology and immunohistochemistry (IHC)

Figure 3.8, shows the histopathological evaluation of the right ear skin, back skin, liver, and spleen. The presence of rete ridges (marked in with red dotted circle) in the right ear and back skin of the positive control group indicated the development of a psoriasis-like condition. Treatment groups did not show rete ridges indicating the effectiveness of clobetasol in treating psoriasis. Psoriatic skin parameters, i.e., hyperkeratosis, parakeratosis, angiogenesis (capillary proliferation), epidermal hyperplasia, suprapappilary thinning, inflammatory infiltrates, munro microabsess and pustule of Kogoj were identified in the samples and scoring was done to determine total skin damage among different groups. It was observed that CP/LPNs-PL gel treated group showed minimum overall skin damage score, which was significantly lower than the Clobetamos^{TM} gel treated group Table 3.3.

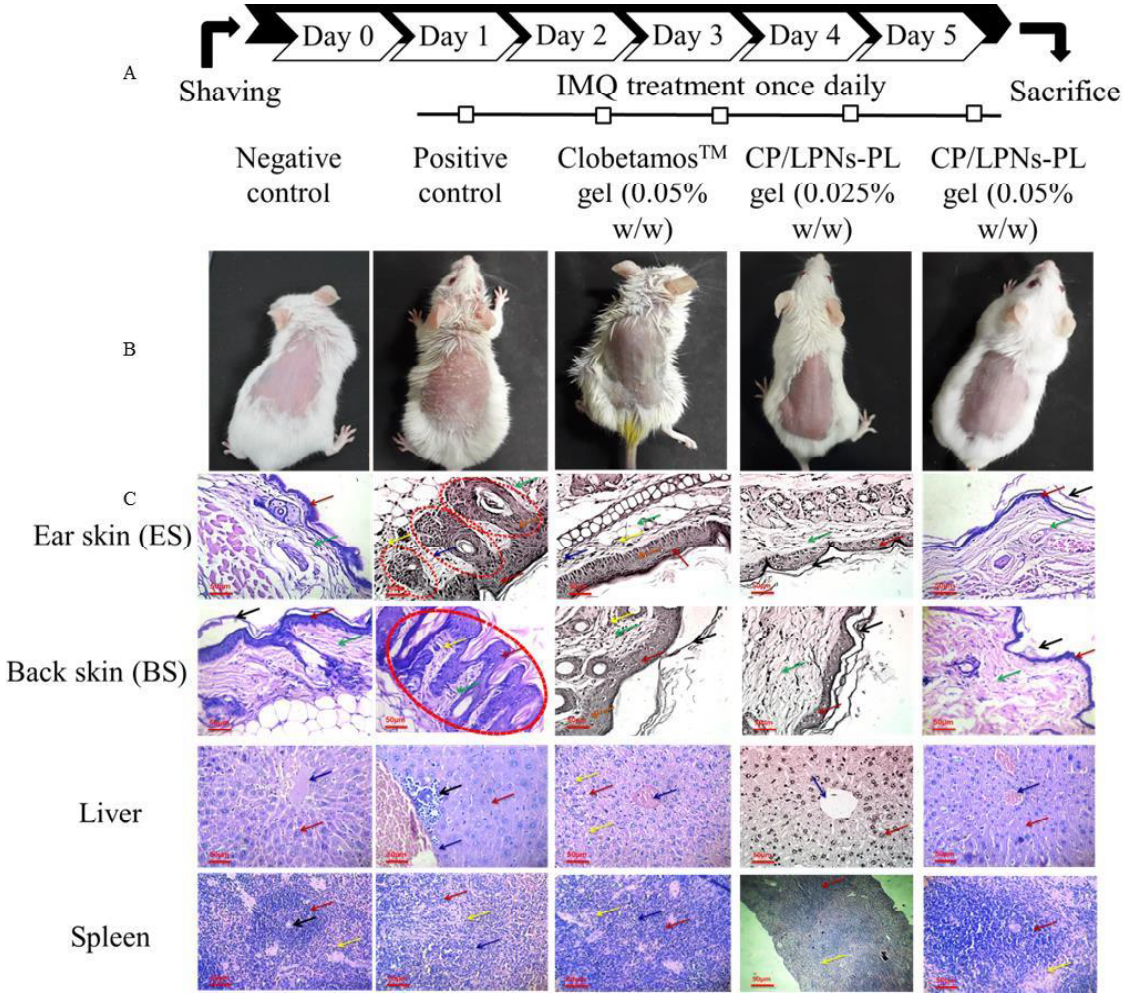

Figure 3.8. IMQ-induced skin inflammation phenotypically simulates psoriasis like skin condition. Swiss albino mice were treated with Imiquad® (5% w/w) on the shaved back skin and right ear on daily basis. (A) Experimental protocol for IMQ-induced psoriasis like mouse model, (B) phenotypical presentation of mouse back skin after 5 days of different treatments, (C) histopathological (H&E staining) evaluation of right ear skin (ES), back skin (BS), liver and spleen of animals at the end of the study. For **ES** and **BS** abbreviations are as follow- **RED Arrow:** Epidermis; **Plain green arrow:** Dermis; **Black arrow:** Stratum corneum**: Yellow Arrow:** Infiltration of inflammatory Cells; **Blue Arrow:** Capillary proliferation; **Orange Arrow:** Epidermal hyperplasia. For **liver** abbreviations are as follow- **RED Arrow:** Hepatocytes; **Black arrow:** Infiltration of mononuclear inflammatory Cells **Yellow Arrow:** Hepatocytes degeneration; **Blue Arrow:** Central vein. For **spleen** abbreviations are as follow- **RED Arrow:** White pulp; **Black arrow:** Splenic central artery **Yellow Arrow:** Red pulp; **Blue Arrow:** Depopulation of lymphocytes in white pulp. (Magnification: 40X). Scale bar = 50 μm.

Table 3.3. Various parameters indicating skin damage score after topical application of Clobetamos™ gel or CP/LPNs-PL gel on the right back of IMQ induced psoriatic mice

Groups	Hyperkeratosis	Parakeratosis	Capillary Proliferation	Epidermal Hyperplasia	Suprapapillary thinning	Inflammatory Infiltrate	Munro microabsess	Pustule of Kogoj	Total skin damage Score
Negative control (ES)	0	0	0	0	0	0	0	0	0
Negative control (BS)	0	0	0	0	0	0	0	0	0
Positive control (ES)	++	++	+	++	+	+	+	0	10
Positive control (BS)	+++	++	+	+++	+	+	0	+	12
Clobetamos ™ gel (0.05% w/w) (ES)	0	0	+	+	0	+	0	0	3
Clobetamos ™ gel (0.05% w/w) (BS)	0	0	+	++	0	+	0	0	4
CP/LPNs-PL gel (0.025% w/w) (ES)	0	0	0	+	0	+	0	0	2
CP/LPNs-PL gel (0.025% w/w) (BS)	0	0	0	+	0	+	0	0	2
CP/LPNs-PL gel (0.05% w/w) (ES)	0	0	+	0	0	0	0	0	1
CP/LPNs-PL gel (0.05% w/w) (BS)	0	0	0	0	0	0	0	0	0

BS- Back skin
ES- Ear skin
'+' indicate mild damage
'++' indicate moderate damage
'+++' indicate severe damage

Histopathology of the liver showed that imiquimod treatment had resulted in hepatocyte degeneration due to the infiltration of inflammatory cells. Clobetasol treatment had shown a reduction of total liver damage score wherein the animals treated with the CP/LPNs-PL gel showed the maximum benefit Table 3.4. In histopathology of the spleen, it was observed that

Table 3.4. Various parameters indicating liver and spleen damage score after topical application of Clobetamos™ gel or CP/LPNs-PL gel on the right back of IMQ induced psoriatic mice

Groups	Infiltration of inflammatory Cells	Degeneration of hepatocyte	Total liver damage Score	Depopulation of Lymphocytes	Total Spleen damage Score
Negative control	0	0	0	0	0
Positive control	+++	++	5	++	2
Clobetamos™ gel (0.05% w/w)	++	+	3	+	1
CP/LPNs-PL gel (0.025% w/w)	+	+	2	+	1
CP/LPNs-PL gel (0.05% w/w)	0	0	0	0	0

'+' indicate mild damage
'++' indicate moderate damage
'+++' indicate severe damage

imiquimod treatment resulted in the rupture of spleenocytes due to the swelling of spleen thereby resulting in the undistinguished red pulp and white pulp areas. Treatment with the CP/LPNs-PL gel had significantly improved the white pulp (blue area) and red pulp (pink area) of the spleen as compared to Clobetamos™ gel treated group with least spleen damage score Table 3.4. There was a difference in the staining intensity observed as the staining were not performed in parallel. However, biasness was avoided by performing an independent blind analysis of the slides.

Further, immuno-histochemistry (IHC) of the back skin showed that Ki-67 protein was highly expressed in the psoriatic skin resulted from the high epidermal cell proliferation. It was observed that animals treated with CP/LPNs-PL gel showed a significant reduction of Ki-67 as compared to the Clobetamos^{TM} gel treated group (Figure 3.9).

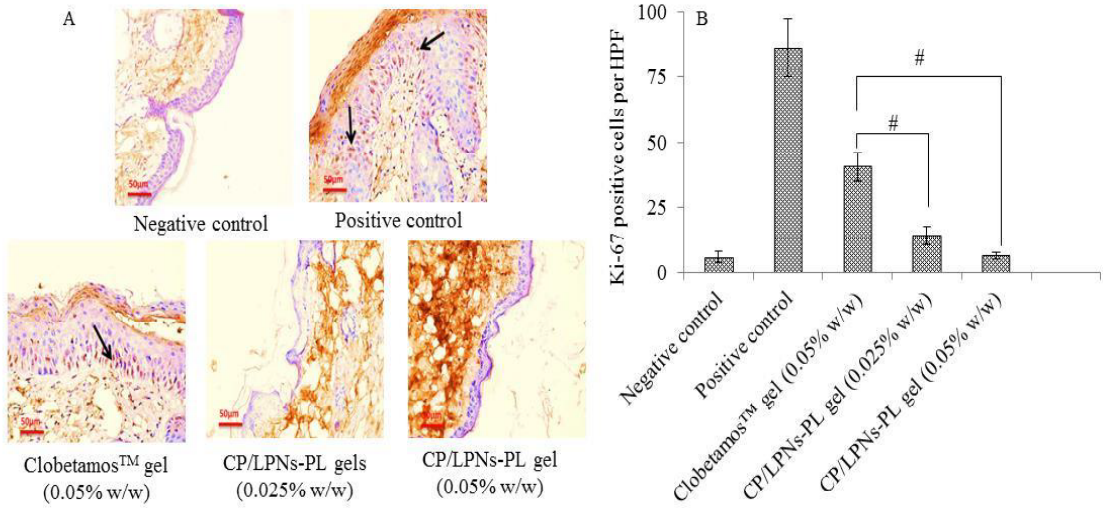

Figure 3.9. (A) Immunohistochemically stained psoriatic back skin sections of mice for Ki-67, cell proliferation marker. CP/LPNs-PL gel treatment could effectively decrease the expression of Ki-67 (Magnification: 40X). Black arrow represents the overexpression of Ki-67. Scale bar = 50 µm. (B) average Ki-67 positive cells per High Power Field (HPF) of different treatment groups. Each value is represented as mean ± SD. #, $p < 0.001$ versus Clobetamos^{TM} gel (0.05% w/w).

4. Discussion

Psoriasis is considered as an autoimmune disorder characterized by erythema, scaling, and thickening of affected skin due to the interaction between activated dendritic cells of the skin and surrounding keratinocytes [6, 7]. Topical corticosteroids are the most preferred medication

for getting symptomatic relief from this inflammatory skin condition; however, they are still associated with both local (such as skin atrophy, skin infections, stretch marks, and redness) and systemic (suppression of hypothalamic-pituitary-adrenal (HPA axis)) side effects. These side effects could be attributed to the high loco-regional concentration of drug and its systemic absorption on application to the skin [11, 12, 20, 21, 23, 24]. To overcome these side-effects, nanoparticles (polymeric and lipidic) offered a viable option by providing a controlled release at the local site, thereby avoiding high loco-regional concentrations [25, 26]. Most of the nanoparticles in literature have shown penetration only into superficial layers of the epidermis but not into deeper layers such as viable epidermis and dermis [72]. Both polymeric and lipid systems have their associated advantages and disadvantages; therefore, newer lipid-polymer hybrid systems have been explored for delivering these therapeutics [33]. Herein, we have demonstrated the potential of lipid-polymer hybrid nanoparticles for delivering a super-potent corticosteroid (clobetasol propionate). There are many nanoparticulate formulations of clobetasol including lipid systems (nanoemulsion, solid lipid nanoparticles and nanostructured lipid carriers) and polymeric systems (nanocapsules and nanospheres) [73-76]. In contrast to the previously reported systems, lipid-polymer hybrid nanoparticles (LPNs) offer several advantages including good drug loading capacities, a more controlled drug release, improved cellular uptake, biocompatibility, and stability [33]. For example, Hu et al. reported the SLNs of clobetasol propionate that exhibited burst release wherein, 45% of drug was released at the end of 3 h. In another study by Nagaich and Gulati, clobetasol propionate loaded nanostructured lipid carriers showed rapid drug release profile, wherein 85% of drug was released at the end of 24 h. In comparison to these, LPNs system imparted sustained drug release profile for over 7 days with no burst release. The strength of this hybrid system also lies in imparting deeper skin penetration

in the viable region along with skin retentive capabilities with negligible systemic leaching. Additionally, *in-vivo* efficacy results demonstrated that even at a half dose, the reported LPNs has a better PASI score as compared to full strength marketed product offering an opportunity for dose reduction and hence the possible reduction of toxicities associated with the corticosteroids.

Several solid lipids, liquid lipids and surfactants were screened to obtain LPNs with smaller size, narrow PDI, and good colloidal stability with high percent encapsulation efficiencies. It was observed that all the three excipients, i.e., solid lipid, liquid lipid, and polymer are essential to obtain stable nanoparticles. Batch 1 and 5 from Table S1 were finalized for making formulations as they showed the desired characteristics. In the preparation of LPNs, mPEG-PLA plays a role in making matrix soft so that it gets dispersed easily on probe sonication and forms nanoparticles with smaller size and narrow PDI. Further, the presence of a hydrophilic mPEG on the surface of the nanoparticles provided the colloidal stability. Among various liquid lipids, unsaturated fatty acids such as linoleic acid and oleic acid showed better encapsulation efficiencies compared to other liquid lipids that could be be due to the presence of double bond in fatty acid chain thereby forming kinks leading to increase in the distance between the fatty acid chains and increased drug loading. In case of solid lipids, precirol and GMS were selected as they yielded dense matrix and produce nanoparticles of good colloidal stability and smaller particle size. Further, the HLB of the surfactant also plays a critical role in nanoparticle assembly. Tween 80 (HLB 15) was able to produce LPNs with higher encapsulation efficiencies and smaller particle size compared to solutol HS 15 (HLB 16.3) and span (HLB 4.3).

Nano-formulations prepared using high pressure homogenization is advantageous from the industry perspective as the process used at lab scale can be scaled-up at commercial level

[77]. It is well established that the high pressure homogenization technique is more efficient compared to ultrasonication [78]. Batches prepared at similar ratio of ingredients by high pressure homogenizer i.e Batch 1 and 2, resulted in smaller particle size with narrow PDI compared to batches processed using probe sonicator (Batch 1 and 5 of Table S1). This could be attributed to the additional mechanisms of size reduction i.e. shear stress and impact forces apart from cavitation. This conclusion is supported by previous research work although it should be noted that the results might be obtained at different values of power/volume ratios. Styrene miniemulsion was prepared by Tang *et al.* using three emulsification devices: (1) Omni mixer (shear), (2) sonifier and (3) Microfluidizer with a similar composition using sodium lauryl sulphate (5 mM) as a surfactant, hexadecane (20 mM) as a costabilizer and styrene (20% w/w). It was observed that final particle size of the emulsion obtained was ranged as $d_{Microfluidizer} < d_{Sonifier} < d_{Omni\ mixer}$ and particle size distribution was narrowest for emulsion prepared by Microfluidizer compared to other equipments [79]. Similar trend of results were observed by Miller *et al.* with Microfluidizer producing smaller droplet size of toluene miniemulsion compared to the sonifier [80]. In high pressure homogenization, extensional force (shear stress) is the major leading force responsible for size reduction with some additional input from cavitation and impact forces. When the coarse dispersion is forced under pressure through a narrow gap at very high velocity, droplets are first elongated in the inlet area followed by disintegration in the turbulent and cavitating flow in the discharge area and are finally impacted on the inner chamber wall. When the dispersion enters the discharge area, there is a large pressure drop resulting into formation of vapor bubbles (cavities) in liquid dispersion that further collapse generating shock waves which produces energy required for breaking droplets [81, 82]. After the size reduction by high pressure homogenizer, the LPNs are subjected to centrifugation at 5000 rpm for 5 min to remove the

larger particles. This may be considered as one of the limitation from the commercialization point of view and further strategies (such as filtration) are warranted in improving the method to avoid the centrifugation step.

Developed nanoparticles were formulated into topical hydrogel using 0.75% w/w Carbopol 974P. This non-benzene grade polymer was selected as a gelling agent because of its highly crosslinked structure that produces gel with high viscosity and desired rheological behavior for topical application. In the formula, propylene glycol served as humectant, while methylparaben and propylparaben were used for their preservative action. Amongst the two selected formulations (Batch 1 and 5 of Table S1), Batch 5 i.e. CP/LPNs-PL produced smaller particle size (128 nm), narrow PDI (0.25) and higher encapsulation (92%) compared to CP/LPNs-GO that demonstrated a particle size of 186 nm with a PDI of 0.35 and encapsulation of 82% when prepared using probe sonication method. Although, there was no significant difference in the particle size between both the formulations prepared by high pressure homogenizer (HPH) however the PDI for CP/LPNs-PL was narrower (0.21) as compared to CP/LPNs-GO (0.27). Further, while preparing the CP/LPNs-GO significant frothing was observed at the stage of mixing by high speed homogenizer. This might be due to the additional emulsifying properties of glyceryl monostearate (GMS). Because of these formulation considerations, CP/LPNs-PL formulation was selected for further evaluation. Successful encapsulation of drug into the central hydrophobic core was confirmed from FTIR and DSC data. FE-SEM and HR-TEM analysis of the gel showed that nanoparticles retained their spherical morphology without any significant aggregation.

Chloroform belongs to Class 2 solvent as per ICH Q3C(R6) guidelines whose level in final products should be limited due to its inherited toxicity. The use of organic solvent could not

be avoided in the preparation method as it is necessary to obtain a uniform matrix. Further the matrixes prepared without chloroform were not dispersible on sonication resulting in the loss of material in the next step. Thus, a minimal amount of chloroform was used in the first step that was subsequently removed from the matrix. While preparing the LPNs, matrix was subjected to heating at 70 °C for 3 h that was sufficient to remove the organic solvent completely. The residual chloroform in the final gel formulation was determined by gas chromatography method that showed undetectable levels indicating complete removal of organic solvent thus avoiding the adverse side effects and possible toxicities associated with it. Our results are in line with Han *et al.* wherein they have determined the residual dichloromethane (Class 2 solvent) in poly(lactide-co-glycolide) nanoparticles by gas chromatography coupled with flame ionization detector [83].

We hypothesized that the hydrophobic block of copolymer together with both solid and liquid lipids forms central hydrophobic core serving two distinct functions: to prevent drug molecules from freely diffusing out of the core, and to reduce the water penetration rate into the core, thereby decreasing the rate of hydrolysis of hydrophobic portion of mPEG-PLA polymers resulting in slower and sustained drug release from the NPs. It has been previously reported that critical values of release exponent 'n' obtained from Korsmeyer–Peppas equation with range 0-0.5 indicates fickian diffusion and if range lies between 0.5-1.0, it supports anomalous or non-fickian diffusion [84, 85]. The herewith reported LPNs exhibited release profile with release exponent 'n' values in the range between 0.5-1.0 indicating that the drug release mechanism was due to combined effect of both diffusion of drug through the hydrophobic core and erosion of matrix justifying the above proposed hypothesis.

Topical pharmaceutical preparations are formulated using various components possessing diverse physico-chemical properties and should exhibit desirable flow properties for achieving

optimal therapeutic benefits. In addition to this, their manufacturing and packaging processes are also closely associated with flow behavior, making rheological studies highly significant [86, 87]. Therefore, the rheological behavior of CP/LPNs-PL gel was evaluated. The rheograms of gel demonstrated a non-Newtonian flow behavior characterized by shear-thinning properties with variable thixotropy which are desirable characteristics for topical formulations, as they facilitate processing during manufacture, packaging, and the flow from the container during usage, spreadability on the skin with improving dermal residence time. Franz diffusion apparatus has been majorly used for performing skin permeation studies. Also USP IV apparatus with dialyze adaptors could also be used for such type of the study. However, out of the available methods for carrying out drug release studies from nanoparticles, dialysis method is also widely reported [51] particularly for the nanoparticle formulations wherein a prolonged drug release is expected. For example, Fontana et al. evaluated clobetasol propionate release from the nanocapsules and nanospheres using dialysis method that showed a drug release over a period of seven to ten days using the DB method [76]. Apart from this, several drug release studies from nanoparticle based formulation (topical applications) used a dialysis method [88-90, 71]. In our study, we have also adopted the dialysis bag method that provided a vital information on the controlled release properties of LPNs [43, 44].

Drug expulsion on storage and during production was a major problem associated with the solid lipid nanoparticles because of crystallization of lipid matrix in less ordered higher energy states during hot homogenization process [91]. This problem of drug expulsion could be overcomed by making the lipid matrix with more imperfections or amorphous. For this, nanostructured lipid carriers (NLCs) have been reported wherein spatial lipids (oils) are used. Although it minimizes the problem of drug expulsion but they tend to shows faster drug release

profiles [33, 92]. In the LPNs, we have used a core made up of hydrophobic component of amphiphilic polymer along with the liquid lipid and solid lipid. This might have resulted in less ordered core that remains stable during storage and hence no drug expulsion was observed for 6 months. Further, the hydrophobicity of the core imparted by the polymer helps in obtaining a sustained release profile even in the presence of a liquid lipid in the core.

Many authorized guidelines have specified the limits of difference factor (f_1) and similarity factor (f_2) which are common parameters used by pharmaceutical industries in predicting the similarity of drug release profiles. For the profiles to be identical f_1 should be in the range of 0-15 and f_2 should be above 50 [93, 94]. In our study, no burst release was observed in the release profiles of CP/LPNs-PL gel after storage for 6 months at room temperature and 2-8 °C indicating that the drug is retained within the core matrix without any drug expulsion. Further, value of difference factor (f_1) was found to be <15 and value of similarity factor (f_2) was found to be >50 indicating that the drug release profiles were identical to that of fresh gel containing LPNs.

Psoriasis pathophysiology involves the proliferation of keratinocytes, leading to the thickening of skin. This could be mimicked in *in vitro* cell cultures using HaCaT cells, which are immortal keratinocyte cells from adult human skin [53]. It has been well reported that effective intracellular drug delivery plays pivotal role in efficacy enhancement by the nanoparticles. These nanoparticles are delivered into the cells by endocytosis process that has been broadly categorized into phagocytosis and pinocytosis. While phagocytosis process most commonly occurs in neutrophils, dendritic cells and macrophages, pinocytosis process occurs in almost all types of cells and can be further subdivided into clathrin-mediated endocytosis, caveolae-mediated endocytosis, lipid-raft mediated endocytosis, clathrin/ caveolae-independent

endocytosis (CIE), and micropinocytosis [54-56]. An understanding of the biological pathway for cellular internalization of the LPNs was studied using four endocytosis inhibitors *viz.* chlorpromazine, mycostatin, methyl-β-cyclodextrin (MβCD), and amiloride. These endocytosis inhibitors are responsible for inhibiting clathrin-mediated endocytosis, caveolae-mediated pathways, lipid raft mediated endocytosis and macropinocytosis, respectively. In our study, the LPNs showed intracellular uptake following lipid-raft and caveolae-mediated mechanism. Luo *et al*. have also reported the macropinocytosis and the caveole pathway for the uptake of liposomes in HaCaT cells [96]. Caveolae (50–80 nm) are flask-shaped invaginations of the cell membrane containing caveolin, which is a dimeric protein that binds to cholesterol, inserts into the plasma membrane as a loop and self-associates to form a caveolin coat on the membrane invaginations. Caveolae-independent endocytosis is not fully understood, however, it requires a 'raft' for internalization and may be defined as raft-/non-caveolae-mediated endocytosis. The literature suggested that, lipid raft and caveolae-mediated endocytic uptake mechanism were able to bypass endo-lysosomal pathways of nanoparticle degradation [97]. Clobetasol propionate has been reported to exhibit anti-proliferative and apoptotic effect on HaCaT cells [57]. We also observed an enhanced *in vitro* cytotoxicity and apoptosis in HaCaT cells after treatment with CP/LPNs-PL that could be attributed due to higher cellular internalization. Further, the cell cycle data suggested a significant arrest of growth of HaCaT cells in S phase.

Ex vivo skin permeation studies were performed using a psoriatic skin from Swiss albino mice. Earlier reports have showed the use of normal skin for studying permeation however the integrity of normal skin and psoriatic skin is very much different. In case of psoriatic skin, the intactness of outer stratum corneum layer is totally altered and thus could show different skin penetration behavior in comparison to normal skin [33]. In our study, LPNs showed penetration

into deeper skin layers such as viable epidermis and dermis with undetectable quantities of drug in receptor compartment indicating no systemic access. This was further supported by undetectable quantities of drug in plasma after topical application of gel containing clobetasol propionate loaded LPNs on *Swiss albino* mice having psoriasis-like inflammation. In contrast to this, topical application of Clobetamos^{TM} gel, a marketed clobetasol propionate gel, resulted into quantifiable plasma levels for up to 6 h after application that may result in undesired systemic side effects. Even though HPLC-MS is a more sensitive system to analyze the drug content. However, we have used a HPLC-UV based method for the bioanalysis of CP that showed no interference with the plasma proteins. Further, it is very important to deliver the drug in the deeper layers of skin (i.e., viable epidermis and dermis) as the skin cell proliferation process initiate from the stratum basale layer of epidermis that is positioned just above the dermis. Viable epidermis is the desired site for drug delivery wherein the drug exerts its therapeutic action. Therefore, the drug in the viable epidermis was analyzed. CP/LPNs showed approximately 12-fold deeper skin penetration compared to Clobetamos^{TM} gel additionally supported by *ex vivo* bioimaging data. Our results are in line with the previous reports, wherein Batheja *et al*. have reported 3.2-fold enhanced permeation of Nile Red in the porcine skin from a HPMC gel containing Nile Red-loaded nanospheres compared to the aqueous Nile Red [98]. In another report it was found that the permeation of Nile red was increased 7 times when incorporated in hyperbranched core-multishell nanocarriers compared to a conventional cream formulation [99].

Application of IMQ on right ear and back skin, lead to increase in the inflammation and resultant increase in the thickness of epidermal tissue due to hyperplasia of keratinocytes. *In vivo* studies conducted on imiquimod induced psoriatic mouse model showed significantly improved PASI parameters (erythema, scaling, thickening and cumulative scoring) in a test group treated

with clobetasol loaded LPNs containing gel (CP/LPNs-PL gel, equivalent to 0.05% w/w) as compared to marketed clobetasol gel (Clobetamos^{TM} gel, equivalent to 0.05% w/w). Further, the size and average weight of spleen of test group treated with CP/LPNs-PL gel (0.05% w/w) was comparable to that of negative control indicating effective treatment. Even at a half dose strength i.e. 0.025% w/w, CP/LPNs-PL gel showed significantly improved PASI parameters, right ear and back skin thickness and average weight of spleen as compared to marketed clobetasol propionate gel (0.05% w/w). Further, histopathological evaluation of right ear, back skin, liver and spleen also showed a reduced total damage score for CP/LPNs-PL gel as compared to marketed clobetasol gel. In psoriatic skin disease, hyper-proliferation of keratinocytes due to inflammatory immune system activation results in an over-expression of Ki-67 protein in a linear fashion of progression of this disease [64, 65]. Immuno-histochemical analysis for Ki-67, an cell proliferation marker showed a significant reduction of average number of Ki-67 nucleoproteins stained per high power field (HPF) in the skin of the animals treated with CP/LPNs-PL gel as compared to marketed clobetasol propionate gel. This enhanced efficacy of the LPNs could be attributed to the deeper skin penetration, higher cellular uptake, slow and pronged drug release with high skin retentive capabilities.

5. Conclusion

In summary, the present work demonstrated LPNs for effective treatment of psoriasis. These LPNs consisted of a solid lipid, liquid lipid and an amphiphilic copolymer, mPEG-PLA. A sustained clobetasol propionate release was obtained from the LPNs gel and were stable at 2-8 °C and room temperature for 6 months with no burst effect. *In vitro* assays on HaCaT cells showed significantly higher uptake of LPNs involving lipid-raft mediated and caveole mediated endocytic uptake mechanism with improved cytotoxicity, apoptosis and cell cycle arrest. Further,

LPNs penetrated into deeper layers of skin, showed no systemic absorption of clobetasol and improved efficacy in IMQ-induced psoriasis-like skin condition in Swiss albino mice. These LPNs could serve as a platform for delivering various hydrophobic potent molecules for skin diseases including cancer, eczema, acne, skin infections, etc and could be translated for clinical evaluation and commercial application.

References

[1] D.G. Stewart, H.M. Lewis, Vitamin D analogues and psoriasis, J Clin Pharm Ther, 21 (1996) 143-148.

[2] B. Limcharoen, P. Pisetpackdeekul, P. Toprangkobsin, P. Thunyakitpisal, S. Wanichwecharungruang, W. Banlunara, Topical Proretinal Nanoparticles: Biological Activities, Epidermal Proliferation and Differentiation, Follicular Penetration, and Skin Tolerability, ACS Biomater Sci Eng, 6 (2020) 1510-1521.

[3] F.C. Eberle, J. Brück, J. Holstein, K. Hirahara, K. Ghoreschi, Recent advances in understanding psoriasis, F1000Res, 5 (2016).

[4] J.E. Hawkes, T.C. Chan, J.G. Krueger, Psoriasis pathogenesis and the development of novel targeted immune therapies, J Allergy Clin Immunol, 140 (2017) 645-653.

[5] C.H. Boakye, K. Patel, R. Doddapaneni, A. Bagde, S. Marepally, M. Singh, Novel amphiphilic lipid augments the co-delivery of erlotinib and Il36 Sirna into the skin for psoriasis treatment, J Control Release, 246 (2017) 120-132.

[6] A.M. Bowcock, J.G. Krueger, Getting under the skin: the immunogenetics of psoriasis, Nat Rev Immunol, 5 (2005) 699-711.

[7] M.A. Lowes, A.M. Bowcock, J.G. Krueger, Pathogenesis and Therapy of Psoriasis, Nature, 445 (2007) 866-873.

[8] R.J. Konrad, R.E. Higgs, G.H. Rodgers, W. Ming, Y.-W. Qian, N. Bivi, J.K. Mack, R.W. Siegel, B.J. Nickoloff, Assessment and Clinical Relevance of Serum Il-19 Levels in Psoriasis and Atopic Dermatitis Using a Sensitive and Specific Novel Immunoassay, Sci Rep, 9 (2019) 1-15.

[9] Y.S. Lee, M.-H. Lee, H.-J. Kim, H.-R. Won, C.-H. Kim, Non-thermal Atmospheric Plasma Ameliorates Imiquimod-induced Psoriasis-like Skin Inflammation in Mice Through Inhibition of Immune Responses and Up-regulation of Pd-l1 Expression, Sci Rep, 7 (2017) 1-12.

[10] Y. Wang, R. Edelmayer, J. Wetter, K. Salte, D. Gauvin, L. Leys, S. Paulsboe, Z. Su, I. Weinberg, M. Namovic, Monocytes/Macrophages Play a Pathogenic Role in Il-23 Mediated Psoriasis-like Skin Inflammation, Sci Rep, 9 (2019) 1-9.

[11] S.R. Feldman, B.A. Yentzer, Topical clobetasol propionate in the treatment of psoriasis, Am J Clin Dermatol, 10 (2009) 397-406.

[12] M. Lebwohl, P. Ting, J. Koo, Psoriasis Treatment: Traditional Therapy, Ann Rheum Dis, 64 (2005) 83-86.

[13] A. Menter, C.E. Griffiths, Current and Future Management of Psoriasis, Lancet, 370 (2007) 272-284.

[14] T. Rhen, J.A. Cidlowski, Antiinflammatory Action of Glucocorticoids—new Mechanisms for Old Drugs, N Engl J Med, 353 (2005) 1711-1723.

[15] M. Perretti, F. D'acquisto, Annexin A1 and Glucocorticoids as Effectors of the Resolution of Inflammation, Nat Rev Immunol, 9 (2009) 62-70.

[16] M.J. García-Pola, L. González-Álvarez, J.M. Garcia-Martin, Treatment of oral lichen planus. Systematic review and therapeutic guide, Med Clin, 149 (2017) 351-362.

[17] M.L. Marnach, R.R. Torgerson, Vulvovaginal issues in mature women, Mayo Clin Proc, 92 (2017) 449-454.

[18] M.A. Gonzalez-Moles, I. Ruiz-Avila, A. Rodriguez-Archilla, P. Morales-Garcia, F. Mesa-Aguado, A. Bascones-Martinez, M. Bravo, Treatment of severe erosive gingival lesions by topical application of clobetasol propionate in custom trays, Oral Surg Oral Med Oral Pathol Oral Radiol, 95 (2003) 688-692.

[19] H.K. Patel, B.S. Barot, P.B. Parejiya, P.K. Shelat, A. Shukla, Topical delivery of clobetasol propionate loaded microemulsion based gel for effective treatment of vitiligo–part II: rheological characterization and in vivo assessment through dermatopharmacokinetic and pilot clinical studies, Colloids Surf B Biointerfaces, 119 (2014) 145-153.

[20] J. Del Rosso, S.F. Friedlander, Corticosteroids: options in the era of steroid-sparing therapy, J Am Acad Dermatol, 53 (2005) S50-S58.

[21] E. Horn, S. Domm, H. Katz, M. Lebwohl, U. Mrowietz, K. Kragballe, I.P. Council, Topical corticosteroids in psoriasis: strategies for improving safety, J Eur Acad Dermatol Venereol, 24 (2010) 119-124.

[22] J. Zhang, E. Smith, Percutaneous Permeation of Betamethasone 17-valerate Incorporated in Lipid Nanoparticles, J Pharm Sci, 100 (2011) 896-903.

[23] H. Schäcke, W.-D. Döcke, K. Asadullah, Mechanisms Involved in the Side Effects of Glucocorticoids, Pharmacol Ther, 96 (2002) 23-43.

[24] J. Vandewalle, A. Luypaert, K. De Bosscher, C. Libert, Therapeutic Mechanisms of Glucocorticoids, Trends Endrocrinol Metab, 29 (2018) 42-54.

[25] P.R. Desai, S. Marepally, A.R. Patel, C. Voshavar, A. Chaudhuri, M. Singh, Topical delivery of anti-TNFα Sirna and capsaicin via novel lipid-polymer hybrid nanoparticles efficiently inhibits skin inflammation in vivo, J Control Release, 170 (2013) 51-63.

[26] P. Desai, R.R. Patlolla, M. Singh, Interaction of nanoparticles and cell-penetrating peptides with skin for transdermal drug delivery, Mol Membr Biol, 27 (2010) 247-259.

[27] T. Şenyiğit, F. Sonvico, S. Barbieri, Ö. Özer, P. Santi, P. Colombo, Lecithin/Chitosan Nanoparticles of Clobetasol-17-propionate Capable of Accumulation in Pig Skin, J Control Release, 142 (2010) 368-373.

[28] L.A.D. Silva, S.F. Taveira, E.M. Lima, R.N. Marreto, In vitro skin penetration of clobetasol from lipid nanoparticles: drug extraction and quantitation in different skin layers, Braz J Pharm Sci, 48 (2012) 811-817.

[29] L. Sun, Z. Liu, L. Wang, D. Cun, H.H. Tong, R. Yan, X. Chen, R. Wang, Y. Zheng, Enhanced Topical Penetration, System Exposure and Anti-psoriasis Activity of Two Particle-sized, Curcumin-loaded Plga Nanoparticles in Hydrogel, J Control Release, 254 (2017) 44-54.

[30] P.P. Shah, P.R. Desai, A.R. Patel, M.S. Singh, Skin Permeating Nanogel for the Cutaneous Co-delivery of Two Anti-inflammatory Drugs, Biomaterials, 33 (2012) 1607-1617.

[31] C.L. Esposito, P. Kirilov, V.G. Roullin, Organogels, promising drug delivery systems: an update of state-of-the-art and recent applications, J Control Release, 271 (2018) 1-20.

[32] L.M. Andrade, L.A.D. Silva, A.P. Krawczyk-Santos, I.C. de SM Amorim, P.B.R. da Rocha, E.M. Lima, J.L.V. Anjos, A. Alonso, R.N. Marreto, S.F. Taveira, Improved tacrolimus skin permeation by co-encapsulation with clobetasol in lipid nanoparticles: study of drug effects in lipid matrix by electron paramagnetic resonance, Eur J Pharm Biopharm, 119 (2017) 142-149.

[33] T. Date, V. Nimbalkar, J. Kamat, A. Mittal, R.I. Mahato, D. Chitkara, Lipid-polymer Hybrid Nanocarriers for Delivering Cancer Therapeutics, J Control Release, 271 (2018) 60-73.

[34] K. Hadinoto, A. Sundaresan, W.S. Cheow, Lipid–polymer Hybrid Nanoparticles as a New Generation Therapeutic Delivery Platform: A Review, Eur J Pharm Biopharm, 85 (2013) 427-443.

[35] B. Mandal, H. Bhattacharjee, N. Mittal, H. Sah, P. Balabathula, L.A. Thoma, G.C. Wood, Core–shell-type Lipid–polymer Hybrid Nanoparticles as a Drug Delivery Platform, Nanomedicine, 9 (2013) 474-491.

[36] J. Cai, H. Huang, W. Song, H. Hu, J. Chen, L. Zhang, P. Li, R. Wu, C. Wu, Preparation and evaluation of lipid polymer nanoparticles for eradicating H. pylori biofilm and impairing antibacterial resistance in vitro, Int J Pharm, 495 (2015) 728-737.

[37] Y. Hu, R. Hoerle, M. Ehrich, C. Zhang, Engineering the lipid layer of lipid–PLGA hybrid nanoparticles for enhanced in vitro cellular uptake and improved stability, Acta Biomater, 28 (2015) 149-159.

[38] J. Shi, Z. Xiao, A.R. Votruba, C. Vilos, O.C. Farokhzad, Differentially Charged Hollow Core/Shell Lipid–polymer–lipid Hybrid Nanoparticles for Small Interfering Rna Delivery, Angew Chem Int Ed, 50 (2011) 7027-7031.

[39] A.-L. Troutier, T. Delair, C. Pichot, C. Ladavière, Physicochemical and Interfacial Investigation of Lipid/Polymer Particle Assemblies, Langmuir, 21 (2005) 1305-1313.

[40] M. Evangelopoulos, A. Parodi, J.O. Martinez, I.K. Yazdi, A. Cevenini, A.L. van de Ven, N. Quattrocchi, C. Boada, N. Taghipour, C. Corbo, Cell source determines the immunological impact of biomimetic nanoparticles, Biomaterials, 82 (2016) 168-177.

[41] C.-M.J. Hu, L. Zhang, S. Aryal, C. Cheung, R.H. Fang, L. Zhang, Erythrocyte membrane-camouflaged polymeric nanoparticles as a biomimetic delivery platform, Proc Natl Acad Sci, 108 (2011) 10980-10985.

[42] I. Aoki, M. Yoneyama, J. Hirose, Y. Minemoto, T. Koyama, D. Kokuryo, R. Bakalova, S. Murayama, T. Saga, S. Aoshima, Thermoactivatable polymer-grafted liposomes for low-invasive image-guided chemotherapy, Transl Res, 166 (2015) 660-673.

[43] V. Dave, K. Tak, A. Sohgaura, A. Gupta, V. Sadhu, K.R. Reddy, Lipid-polymer hybrid nanoparticles: Synthesis strategies and biomedical applications, J Microbiol Methods, 160 (2019) 130-142.

[44] B. Mandal, H. Bhattacharjee, N. Mittal, H. Sah, P. Balabathula, L.A. Thoma, G.C. Wood, Core–shell-type lipid–polymer hybrid nanoparticles as a drug delivery platform, Nanomedicine, 9 (2013) 474-491.

[45] S. Krishnamurthy, R. Vaiyapuri, L. Zhang, J.M. Chan, Lipid-coated Polymeric Nanoparticles for Cancer Drug Delivery, Biomater Sci, 3 (2015) 923-936.

[46] R.J. Bose, R. Ravikumar, V. Karuppagounder, D. Bennet, S. Rangasamy, R.A. Thandavarayan, Lipid–polymer hybrid nanoparticle-mediated therapeutics delivery: advances and challenges, Drug Discov Today, 22 (2017) 1258-1265.

[47] R.H. Fang, K.N. Chen, S. Aryal, C.-M.J. Hu, K. Zhang, L. Zhang, Large-scale synthesis of lipid–polymer hybrid nanoparticles using a multi-inlet vortex reactor, Langmuir, 28 (2012) 13824-13829.

[48] Y. Kim, B. Lee Chung, M. Ma, W.J. Mulder, Z.A. Fayad, O.C. Farokhzad, R. Langer, Mass Production and Size Control of Lipid–polymer Hybrid Nanoparticles Through Controlled Microvortices, Nano Lett, 12 (2012) 3587-3591.

[49] C. Zhang, L. Liao, S. Gong, Microwave-Assisted Synthesis of PLLA-PEG-PLLA Triblock Copolymers, Macromol Rapid Commun, 28 (2007) 422-427.

[50] M. Alibolandi, F. Sadeghi, S.H. Sazmand, S.M. Shahrokhi, M. Seifi, F. Hadizadeh, Synthesis and self-assembly of biodegradable polyethylene glycol-poly (lactic acid) diblock copolymers as polymersomes for preparation of sustained release system of doxorubicin, Int J Pharm Investig, 5 (2015) 134.

[51] V. Gupta, P. Trivedi, In vitro and in vivo characterization of pharmaceutical topical nanocarriers containing anticancer drugs for skin cancer treatment, Lipid nanocarriers for drug targeting, (2018) 563-627.

[52] Y. Zhang, M. Huo, J. Zhou, A. Zou, W. Li, C. Yao, S. Xie, DDSolver: an add-in program for modeling and comparison of drug dissolution profiles, AAPS J, 12 (2010) 263-271.

[53] D. Breitkreutz, P. Boukamp, C.M. Ryle, H.-J. Stark, D.R. Roop, N.E. Fusenig, Epidermal morphogenesis and keratin expression in C-ha-ras-transfected tumorigenic clones of the human Hacat cell line, Cancer Res, 51 (1991) 4402-4409.

[54] H.P. Lin, B. Singla, P. Ghoshal, J.L. Faulkner, M. Cherian-Shaw, P.M. O'Connor, J.X. She, E.J. Belin de Chantemele, G. Csányi, Identification of Novel Macropinocytosis Inhibitors Using a Rational Screen of Food and Drug Administration-approved Drugs, Br J Pharmacol, 175 (2018) 3640-3655.

[55] D. Dutta, J.G. Donaldson, Search for inhibitors of endocytosis: intended specificity and unintended consequences, Cell Logist, 2 (2012) 203-208.

[56] M. Koivusalo, C. Welch, H. Hayashi, C.C. Scott, M. Kim, T. Alexander, N. Touret, K.M. Hahn, S. Grinstein, Amiloride Inhibits Macropinocytosis by Lowering Submembranous Ph and Preventing Rac1 and Cdc42 Signaling, J Cell Biol, 188 (2010) 547-563.

[57] A. Guichard, P. Humbert, M. Tissot, P. Muret, C. Courderot-Masuyer, C. Viennet, Effects of topical corticosteroids on cell proliferation, cell cycle progression and apoptosis: in vitro comparison on Hacat, Int J Pharm, 479 (2015) 422-429.

[58] L. Nerurkar, A. McColl, G. Graham, J. Cavanagh, The Systemic Response to Topical Aldara Treatment Is Mediated Through Direct Tlr7 Stimulation as Imiquimod Enters the Circulation, Sci Rep, 7 (2017) 1-11.

[59] J.Y. Kim, J. Ahn, J. Kim, M. Choi, H. Jeon, K. Choe, D.Y. Lee, P. Kim, S. Jon, Nanoparticle-assisted transcutaneous delivery of a signal transducer and activator of transcription 3-inhibiting peptide ameliorates psoriasis-like skin inflammation, ACS Nano, 12 (2018) 6904-6916.

[60] N.-W. Kang, M.-H. Kim, S.-Y. Sohn, K.-T. Kim, J.-H. Park, S.-Y. Lee, J.-Y. Lee, D.-D. Kim, Curcumin-loaded lipid-hybridized cellulose nanofiber film ameliorates imiquimod-induced psoriasis-like dermatitis in mice, Biomaterials, 182 (2018) 245-258.

[61] S. Jain, R. Addan, V. Kushwah, H. Harde, R.R. Mahajan, Comparative assessment of efficacy and safety potential of multifarious lipid based Tacrolimus loaded nanoformulations, Int J Pharm., 562 (2019) 96-104.

[62] B. N'Dri-Stempfer, W.C. Navidi, R.H. Guy, A.L. Bunge, Improved bioequivalence assessment of topical dermatological drug products using dermatopharmacokinetics, Pharm Res, 26 (2009) 316.

[63] T. Ângelo, M.S. Cunha-Filho, G.M. Gelfuso, T. Gratieri, Chromatographic method for clobetasol propionate determination in hair follicles and in different skin layers, Biomed Chromatogr, 31 (2017) e3804.

[64] Y. Chen, Q. Zhang, H. Liu, C. Lu, C.-L. Liang, F. Qiu, L. Han, Z. Dai, Esculetin ameliorates psoriasis-like skin disease in mice by inducing Cd4+ Foxp3+ regulatory T cells, Front Immunol, 9 (2018) 2092.

[65] M. Xu, H. Lu, Y.-H. Lee, Y. Wu, K. Liu, Y. Shi, H. An, J. Zhang, X. Wang, Y. Lai, An Interleukin-25-mediated Autoregulatory Circuit in Keratinocytes Plays a Pivotal Role in Psoriatic Skin Inflammation, Immunity, 48 (2018) 787-798. e4.

[66] S. Kaddu, S. Hodl, H. Soyer, Histopathologic spectrum of psoriasis, Acta Dermatovenerol Alp Pannonica Adriat, 8 (1999) 94-99.

[67] B.Y. Kim, J.W. Choi, B.R. Kim, S.W. Youn, Histopathological findings are associated with the clinical types of psoriasis but not with the corresponding lesional psoriasis severity index, Ann Dermatol, 27 (2015) 26-31.

[68] P. Vasseur, M. Pohin, J. Jégou, L. Favot, N. Venisse, J. Mcheik, F. Morel, J. Lecron, C. Silvain, Liver Fibrosis Is Associated with Cutaneous Inflammation in the Imiquimod-induced Murine Model of Psoriasiform Dermatitis, Br J Dermatol, 179 (2018) 101-109.

[69] S. Horváth, R. Komlódi, A. Perkecz, E. Pintér, R. Gyulai, Á. Kemény, Methodological refinement of aldara-induced psoriasiform dermatitis model in mice, Sci Rep, 9 (2019) 1-8.

[70] P. Sakdiset, T. Amnuaikit, W. Pichayakorn, S. Pinsuwan, Formulation development of ethosomes containing indomethacin for transdermal delivery, J Drug Deliv Sci Technol, 52 (2019) 760-768.

[71] A. Essaghraoui, A. Belfkira, B. Hamdaoui, C. Nunes, S.A.C. Lima, S. Reis, Improved dermal delivery of cyclosporine a loaded in solid lipid nanoparticles, Nanomaterials, 9 (2019) 1204.

[72] F. Rancan, Q. Gao, C. Graf, S. Troppens, S. Hadam, S. Hackbarth, C. Kembuan, U. Blume-Peytavi, E. Rühl, J.r. Lademann, Skin Penetration and Cellular Uptake of Amorphous Silica Nanoparticles with Variable Size, Surface Functionalization, and Colloidal Stability, ACS Nano, 6 (2012) 6829-6842.

[73] M.S. Alam, M.S. Ali, N. Alam, M.R. Siddiqui, M. Shamim, M. Safhi, In vivo study of clobetasol propionate loaded nanoemulsion for topical application in psoriasis and atopic dermatitis, Drug Invent Today, 5 (2013) 8-12.

[74] F. Hu, H. Yuan, H. Zhang, M. Fang, Preparation of solid lipid nanoparticles with clobetasol propionate by a novel solvent diffusion method in aqueous system and physicochemical characterization, Int J Pharm, 239 (2002) 121-128.

[75] U. Nagaich, N. Gulati, Nanostructured lipid carriers (NLC) based controlled release topical gel of clobetasol propionate: design and in vivo characterization, Drug Deliv Transl Res, 6 (2016) 289-298.

[76] M. Fontana, K. Coradini, S. Guterres, A. Pohlmann, R. Beck, Nanoencapsulation as a way to control the release and to increase the photostability of clobetasol propionate: influence of the nanostructured system, J Biomed Nanotechnol, 5 (2009) 254-263.

[77] M. Durán-Lobato, A. Enguix-González, M. Fernández-Arévalo, L. Martín-Banderas, Statistical analysis of solid lipid nanoparticles produced by high-pressure homogenization: a practical prediction approach, J Nanopart Res, 15 (2013) 1443.

[78] J.M. Asua, Miniemulsion polymerization, Prog Polym Sci, 27 (2002) 1283-1346.

[79] E.S. Daniels, E.D. Sudol, M.S. El-Aasser, Polymer latexes: preparation, characterization, and applications, Washington, DC (United States); American Chemical Society, 1992.

[80] C. Miller, J. Venkatesan, C. Silebi, E. Sudol, M. El-Aasser, Characterization of Miniemulsion Droplet Size and Stability Using Capillary Hydrodynamic Fractionation, J Colloid Interface Sci, 162 (1994) 11-18.

[81] S.I. Martínez-Monteagudo, B. Yan, V. Balasubramaniam, Engineering Process Characterization of High-pressure Homogenization—from Laboratory to Industrial Scale, Food Eng Rev, 9 (2017) 143-169.

[82] V. Gall, M. Runde, H.P. Schuchmann, Extending applications of high-pressure homogenization by using simultaneous emulsification and mixing (Sem)—an overview, Processes, 4 (2016) 46.

[83] E.-J. Han, A.-H. Chung, I.-J. Oh, Analysis of residual solvents in poly (lactide-co-glycolide) nanoparticles, J Pharm Invest, 42 (2012) 251-256.

[84] D.L. Sitta, M.R. Guilherme, E.P. da Silva, A.J. Valente, E.C. Muniz, A.F. Rubira, Drug Release Mechanisms of Chemically Cross-linked Albumin Microparticles: Effect of the Matrix Erosion, Colloids Surf B Biointerfaces, 122 (2014) 404-413.

[85] R. Jain, S.K. Sukla, N. Nema, A. Panday, Drug nano-particle: A release kinetics, J Nanomed Nanotechnol, 6 (2015) 1.

[86] S. El-Housiny, M.A. Shams Eldeen, Y.A. El-Attar, H.A. Salem, D. Attia, E.R. Bendas, M.A. El-Nabarawi, Fluconazole-loaded solid lipid nanoparticles topical gel for treatment of Pityriasis versicolor: formulation and clinical study, Drug Deliv, 25 (2018) 78-90.

[87] A. Walicka, J. Falicki, B. Iwanowska-Chomiak, Rheology of drugs for topical and transdermal delivery, Int J Appl Mech Eng, 24 (2019) 179-198.

[88] M.F. Pinto, C.C. Moura, C. Nunes, M.A. Segundo, S.A.C. Lima, S. Reis, A new topical formulation for psoriasis: development of methotrexate-loaded nanostructured lipid carriers, Int J Pharm, 477 (2014) 519-526.

[89] D. Fathalla, E.M. Youssef, G.M. Soliman, Liposomal and Ethosomal Gels for the Topical Delivery of Anthralin: Preparation, Comparative Evaluation and Clinical Assessment in Psoriatic Patients, Pharmaceutics, 12 (2020) 446.

[90] R. Sonawane, H. Harde, M. Katariya, S. Agrawal, S. Jain, Solid lipid nanoparticles-loaded topical gel containing combination drugs: an approach to offset psoriasis, Expert Opin Drug Deliv, 11 (2014) 1833-1847.

[91] V. Mishra, K.K. Bansal, A. Verma, N. Yadav, S. Thakur, K. Sudhakar, J.M. Rosenholm, Solid Lipid Nanoparticles: Emerging Colloidal Nano Drug Delivery Systems, Pharmaceutics, 10 (2018) 191.

[92] A. Puri, K. Loomis, B. Smith, J.-H. Lee, A. Yavlovich, E. Heldman, R. Blumenthal, Lipid-based Nanoparticles as Pharmaceutical Drug Carriers: From Concepts to Clinic, Crit Rev Ther Drug Carrier Syst, 26 (2009).

[93] D.A. Diaz, S.T. Colgan, C.S. Langer, N.T. Bandi, M.D. Likar, L. Van Alstine, Dissolution similarity requirements: how similar or dissimilar are the global regulatory expectations?, AAPS J, 18 (2016) 15-22.

[94] R.E. Stevens, V. Gray, A. Dorantes, L. Gold, L. Pham, Scientific and Regulatory Standards for Assessing Product Performance Using the Similarity Factor, F2, AAPS J, 17 (2015) 301-306.

[95] A. Mielanczyk, K. Mrowiec, M. Kupczak, Ł. Mielanczyk, D. Scieglinska, A. Gogler-Piglowska, M. Michalski, A. Gabriel, D. Neugebauer, M. Skonieczna, Synthesis and in vitro

cytotoxicity evaluation of star-shaped polymethacrylic conjugates with methotrexate or acitretin as potential antipsoriatic prodrugs, Eur J Pharmacol, 866 (2020) 172804.

[96] H.-C. Luo, N. Li, L. Yan, K.-j. Mai, K. Sun, W. Wang, G.-J. Lao, C. Yang, L.-M. Zhang, M. Ren, Comparison of the Cellular Transport Mechanism of Cationic, Star-shaped Polymers and Liposomes in Hacat Cells, Int J Nanomed, 12 (2017) 1085.

[97] I.-L. Hsiao, A.M. Gramatke, R. Joksimovic, M. Sokolowski, M. Gradzielski, A. Haase, Size and cell type dependent uptake of silica nanoparticles, J Nanomed Nanotechnol, 5 (2014).

[98] P. Batheja, L. Sheihet, J. Kohn, A.J. Singer, B. Michniak-Kohn, Topical drug delivery by a polymeric nanosphere gel: formulation optimization and in vitro and in vivo skin distribution studies, J Control Release, 149 (2011) 159-167.

[99] F. Du, S. Hönzke, F. Neumann, J. Keilitz, W. Chen, N. Ma, S. Hedtrich, R. Haag, Development of biodegradable hyperbranched core-multishell nanocarriers for efficient topical drug delivery, J Control Release, 242 (2016) 42-49.